DOI: 10.1002/chem.201200159

Iron Borohydride Pincer Complexes for the Efficient Hydrogenation of Ketones under Mild, Base-Free Conditions: Synthesis and Mechanistic Insight

Robert Langer,[a] Mark A. Iron,[b] Leonid Konstantinovski,[b] Yael Diskin-Posner,[b] Gregory Leitus,[b] Yehoshoa Ben-David,[a] and David Milstein*[a]

Abstract: The new, structurally characterized hydrido carbonyl tetrahydridoborate iron pincer complex [(*i*Pr-PNP)Fe(H)(CO)(η^1-BH_4)] (**1**) catalyzes the base-free hydrogenation of ketones to their corresponding alcohols employing only 4.1 atm hydrogen pressure. Turnover numbers up to 1980 at complete conversion of ketone were reached with this system. Treatment of **1** with aniline (as a BH_3 scavenger) resulted in a mixture of *trans*-[(*i*Pr-PNP)Fe(H)$_2$(CO)] (**4a**) and *cis*-[(*i*Pr-PNP)Fe(H)$_2$(CO)] (**4b**). The dihydrido complexes **4a** and **4b** do not react with acetophenone or benzaldehyde, indicating that these complexes are not intermediates in the catalytic reduction of ketones. NMR studies indicate that the tetrahydridoborate ligand in **1** dissociates prior to ketone reduction. DFT calculations show that the mechanism of the iron-catalyzed hydrogenation of ketones involves alcohol-assisted aromatization of the dearomatized complex [(*i*Pr-PNP*)Fe(H)(CO)] (**7**) to initially give the Fe^0 complex [(*i*Pr-PNP)Fe(CO)] (**21**) and subsequently [(*i*Pr-PNP)Fe(CO)(EtOH)] (**38**). Concerted coordination of acetophenone and dual hydrogen-atom transfer from the PNP arm and the coordinated ethanol to, respectively, the carbonyl carbon and oxygen atoms, leads to the dearomatized complex [(*i*Pr-PNP*)Fe(CO)(EtO)(MeCH(OH)Ph)] (**32**). The catalyst is regenerated by release of 1-phenylethanol, followed by dihydrogen coordination and proton transfer to the coordinated ethoxide ligand.

Keywords: density functional calculations · homogeneous catalysis · hydrogenation · iron · pincer ligands

Introduction

The replacement of precious noble metal catalysts by inexpensive and environmentally benign metals is a desirable goal in chemistry. Iron complexes in particular would provide an excellent alternative, due to the high natural abundance and low toxicity of iron.[1] Although considerable progress has been made recently in various iron-catalyzed reactions,[1c,2–6] the development of efficient iron catalysts for clean and environmentally friendly transformations remains a big challenge.

The hydrogenation of polar and apolar multiple bonds, typically catalyzed by Ru, Rh and Ir complexes, is an atom economical synthetic method.[7] While iron-catalyzed hydrosilylations and transfer hydrogenations have been demonstrated in a number of cases,[3] only a few examples of reductions with hydrogen gas are described in the literature. Importantly, Chirik and co-workers described the hydrogenation of simple alkenes and alkynes under mild conditions, using 0.3 mol% of the well defined Fe^0 dinitrogen complex [(*i*Pr-PDI)Fe(N$_2$)$_2$] (*i*Pr-PDI = ((2,6-CHMe$_2$)$_2$C$_6$H$_3$N=CMe)$_2$C$_5$H$_3$N).[4] With turnover frequencies of 1814 h^{-1}, this iron complex gave even better results than common homogeneous and heterogeneous noble metal catalysts, such as Pd/C, [RhCl(PPh$_3$)$_3$] or [Ir(cod)(PCy$_3$)(py)]PF$_6$. The first example of an iron-catalyzed hydrogenation of ketones or aldehydes was described by Casey et al., using the bifunctional [(2,5-(SiMe$_3$)$_2$-3,4-(CH$_2$)$_4$(η^5-C$_4$COH)Fe(CO)$_2$H] complex.[5] This complex catalyzes the hydrogenation of ketones and aldehydes with high chemo- and diastereoselectivity, with turnover numbers up to 50, employing three atmospheres of hydrogen pressure at ambient temperature. The tetradentate diiminodiphosphine and diaminodiphosphine iron complexes, reported by Morris and co-workers, efficiently catalyze the hydrogenation of acetophenone with high conversion at high pressure and excess of base (T = 50 °C, p(H$_2$) = 25 atm, TON 225; catalyst/base = 15).[6]

We recently reported a highly efficient hydrogenation of ketones catalyzed by an iron pincer complex in the presence

[a] Dr. R. Langer, Y. Ben-David, Prof. Dr. D. Milstein
Department of Organic Chemistry
Weizmann Institute of Science
76100 Rehovot (Israel)
Fax: (+972)-8-934-4142
E-mail: david.milstein@weizmann.ac.il

[b] Dr. M. A. Iron, Dr. L. Konstantinovski, Dr. Y. Diskin-Posner, Dr. G. Leitus
Department of Chemical Research Support
Weizmann Institute of Science
76100 Rehovot (Israel)

Supporting information for this article is available on the WWW under http://dx.doi.org/10.1002/chem.201200159.

of catalytic amounts of base.[8] A new mode of cooperation between the metal center and the pincer ligand, which has been observed for the corresponding ruthenium complexes,[9] is likely responsible for the high catalytic activity of the iron complex. In order to make this transformation even more efficient, it would be desirable to obviate the need for added base. Ruthenium hydrido tetrahydridoborate complexes were demonstrated to efficiently catalyze the hydrogenation of organic carbonyl compounds.[10] The use of analogous iron(II) complexes for the base free hydrogenation of ketones was deemed worthy of investigation. Reported examples of iron tetrahydridoborate complexes are not common and the simple homoleptic $Fe(BH_4)_2$ is only stable below −10 °C.[11] While mononuclear and polynuclear iron complexes with η^1-,[12] η^2-[13,14] and η^3-coordinated[15] tetrahydridoborate, as well as complexes with bridging hexahydridoborate,[16] ligands have been reported, we are aware of only two mononuclear and structurally characterized hydrido tetrahydridoborate iron complexes.[12,14]

Herein we report the synthesis and characterization of the hydrido tetrahydridoborate iron pincer complexes [(*i*Pr-PNP)Fe(H)(CO)(η^1-BH_4)] (**1**) and [(*i*Pr-PNP)Fe(H)(η^2-BH_4)] (**2**). Both complexes were investigated as pre-catalysts for the hydrogenation of ketones under base-free conditions. Complex **1** shows similar activity as the previously reported pre-catalyst [(*i*Pr-PNP)Fe(H)(CO)(Br)] (**3**), but unlike the latter complex, the addition of a strong base is not required. The reaction takes place under mild conditions, with turnover numbers up to 1980 and turnover frequencies up to 330 h^{-1} at complete conversion of ketone, employing 4.1 atm of hydrogen pressure at 40 °C. In addition, we have developed a deeper mechanistic understanding of iron-catalyzed ketone hydrogenation, via a series of stoichiometric reactions of complex **1** and by density functional theory (DFT) calculations.

Results and Discussion

Treatment of [(*i*Pr-PNP)Fe(CO)Br_2] with an excess of $NaBH_4$ (5 equivalents) results in the formation of the hydrido borohydride complex **1** in good yield (Scheme 1). The $^{31}P\{^1H\}$ NMR spectrum exhibits a singlet resonance at $\delta =$ 93.57 ppm, consistent with two equivalent phosphorus centers. The methyl protons of the isopropyl groups give rise to four doublets of doublets in the ^1H NMR at $\delta = 0.76$, 1.17, 1.23 and 1.49 ppm indicating the absence of C_s or C_2 symmetry. In addition, a sharp triplet at $\delta = -16.62$ ppm for the coordinated hydride and a broad resonance at $\delta = -2.29$ ppm that integrates to four protons for the coordinated borohydride ligand are observed in the ^1H NMR spectrum. The observation of a broad four proton resonance in this region of the ^1H NMR spectrum is typical for η^1-coordinated borohydride complexes of iron and ruthenium and indicates a dynamic behavior of the coordinated borohydride ligand.[17] Absorptions at 2318 and 2269 cm^{-1} in the IR spectrum for the terminal and at 2028 cm^{-1} for the bridging hydrogen atoms support an η^1-binding mode of the borohydride ligand. The X-ray crystal structure of **1** (Figure 1) reveals a distorted octahedral coordination geometry around the Fe^{II} center, with the CO ligand located *trans* to the pyridine nitrogen and the hydride ligand located *trans* to the η^1-coordinated borohydride ligand. The Fe1–B1 distance (2.67 Å) in **1** is shorter than in the previously described iron hydrido borohydride complex [$(dmpe)_2FeH(\eta^1$-$BH_4)$] (2.84 Å, dmpe = 1,2-bis(dimethylphosphino)ethane),[12] indicating a stronger bond between the iron(II) center and the borohydride ligand.

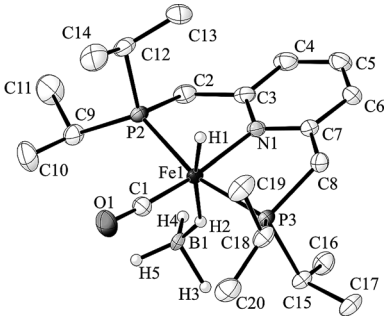

Figure 1. Molecular structure of complex **1** with the thermal ellipsoids set at 50% probability. Selected bond lengths [Å] and angles [°]: Fe1–P2 2.204(1), Fe1–P3 2.204(1), Fe1–N1 2.038(1), Fe–C1 1.728(2), Fe1–H1 1.43(2), Fe1–H2 1.615, O1–C1 1.161(2), B1–H2 1.180, B1–H3 1.270, B–H4 1.233, B1–H5 1.079, P2-Fe1-P3 164.46(2), Fe1-C1-O1 175.10(14), N1-Fe1-C1 170.04(6), H1-Fe1-H2 169.7, H2-B1-H3 102.3, H2-B1-H4 117.0, H2-B1-H5 131.0, H3-B1-H4 103.5, H3-B1-H5 96.5, H4-B1-H5 101.6, Fe1-H2-B1 144.75.

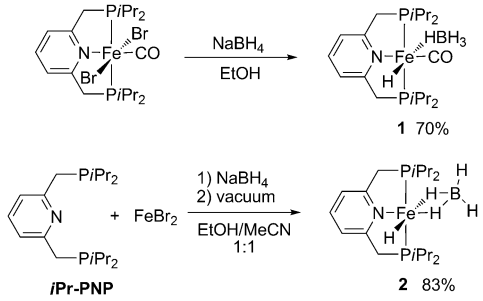

Scheme 1. Synthesis of iron hydrido borohydride complexes.

Addition of an excess of $NaBH_4$ (4 equivalents) to a solution of $FeBr_2$ and *i*Pr-PNP in a 1:1 mixture of acetonitrile and ethanol leads immediately to a deep red solution. Evaporation of the reaction mixture followed by extraction with pentane yields the hydrido borohydride complex **2**. The $^{31}P\{^1H\}$ NMR of **2** exhibits a singlet resonance at $\delta =$ 97.68 ppm indicating the equivalence of both phosphorus centers. A sharp triplet is observed for the hydride ligand at $\delta = -18.18$ ppm in the ^1H NMR, while the borohydride ligand gives rise to two broad proton signals at $\delta = -28.67$ and −9.63 ppm for the bridging hydrogen atoms and a broad doublet at $\delta = 4.95$ ppm that integrates to two pro-

tons for the terminal hydrogens. This splitting of the protons in the ^{1}H NMR spectrum is typically observed for η^2-coordinated borohydrides. The observation of strong bands at 2387 and 2322 cm^{-1} in the IR spectrum for the B–H vibrations of the terminal hydrides and a broad band at 1818 cm^{-1} confirms an η^2-binding mode of the borohydride ligand.[17] The X-ray crystal structure of **2** shows that the iron(II) center is in a distorted octahedral environment (Figure 2). The Fe–B distance of 2.095(3) Å is consistent with a η^2-binding mode of the borohydride ligand.

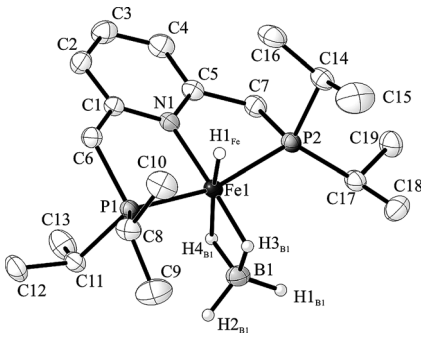

Figure 2. Molecular structure of complex **2** with the thermal ellipsoids set at 50% probability. Selected bond lengths [Å] and angles [°]: Fe1–P1 2.169(1), Fe1–P2 2.183(1), Fe1–N1 1.974(2), Fe1–$H1_{Fe}$ 1.48(2), Fe1–$H3_{B1}$ 1.60(2), Fe1–H4B1 1.68(2), B1–H1B1 1.10(2), B1–$H3_{B1}$ 1.25(2), B1–$H4_{B1}$ 1.28(2), B1–$H2_{B1}$ 1.13(2), P1-Fe1-P2 163.5(1), $H1_{Fe}$-Fe1-$H3_{B1}$ 95.9(12), $H1_{Fe}$-Fe1-$H4_{B1}$ 170.0(12), $H3_{B1}$-Fe1-$H4_{B1}$ 74.1(11), $H2_{B1}$-B1-$H4_{B1}$ 110.1(15), $H3_{B1}$-B1-$H4_{B1}$ 103.1(14), $H1_{B1}$-B1-$H2_{B1}$ 111.6(16), $H1_{B1}$-B1-$H3_{B1}$ 109.6(15), $H1_{B1}$-B1-$H4_{B1}$ 111.0(15), $H2_{B1}$-B1-$H3_{B1}$ 111.2(14).

The borohydride complexes **1** and **2** were investigated as pre-catalysts in the hydrogenation of acetophenone without any added base, utilizing 0.05 mol% complex, 4.1 atm hydrogen and ethanol as the solvent (Table 1). At ambient temperature with complex **1**, *rac*-1-phenylethanol was obtained in a poor yield of 12%. However, at 40 °C complex **1** showed comparable catalytic activity to the previously reported [(*i*Pr-PNP)Fe(CO)(H)Br] (**3**) system,[8] while the hydrido borohydride complex **2** displayed no activity at all.

Catalyst **1** was tested for a number of substrates under various reaction conditions (Table 2). Complete conversion of acetophenone to *rac*-1-phenylethanol was observed when a slightly higher loading of **1** was employed (Table 2, entry 2). Halogen-substituted acetophenones were hydrogenated in high yields and, importantly, no hydrogenolysis of the carbon–halogen bonds took place (Table 2, entries 3 and 4). The methyl-substituted derivative was reduced to the corresponding alcohol in moderate yield (Table 2, entry 5). Hydrogenation of cyclohexanone resulted in the formation of the corresponding alcohol in 44% yield (Table 2, entry 6), while benzophenone was hydrogenated in 72% yield (Table 2, entry 7). Since the latter compound is not enolizable, it is unlikely that in the case of enolizable ketones hydrogenation of the carbon–carbon double bond of the corresponding enol is significantly involved.

Table 1. Hydrogenation of acetophenone.[a]

Complex	T [°C]	t [h]	Yield [%] (conversion)[b]	TON	TOF [h^{-1}]
1	26	21	12 (12)	240	11
1	40	6	89 (89)	1780	296
2	40	6	0	0	0
3[c]	26	21	94 (94)	1880	89
3[c]	40	4	85 (86)	1700	425

[a] Reaction conditions: Complex (0.0025 mmol), acetophenone (5 mmol), *m*-xylene (1 mmol), ethanol (3 mL), H_2 (4.1 atm), 40 °C. [b] Determined by GC analysis with *m*-xylene as internal standard. [c] 0.005 mmol KO*t*Bu were added (For details, see ref. [8]).

The hydrogenation of benzil resulted in the formation of benzoin in surprisingly poor yields (Table 2, entry 8). 2-Acetylpyridine was completely converted to *rac*-1-(pyridin-2-yl)ethanol with the highest turnover number reported so far for an iron-catalyzed hydrogenation of a ketone (Table 2, entry 9, TON = 1980). Complex **1** displayed increased activity in the hydrogenation of α,β-unsaturated ketones, such as *trans*-4-phenyl-3-buten-2-one, in which case reduction of the carbon–carbon double bond also took place (Table 2, entry 10). Hydrogenation of aldehydes is problematic. Only traces of benzyl alcohol were observed, but this process could be somewhat facilitated by the addition of base (Table 2, entry 11).

We have previously proposed that the catalytic hydrogenation of ketones by **3** in the presence of a catalytic amount of base involves the formation of a dearomatized pentacoordinated intermediate as the initial step in the catalytic cycle, and that this intermediate is stabilized by reversible addition of ethanol.[8] We demonstrated that the addition of hydrogen to a dearomatized complex (stabilized by a donor ligand) led to a dihydride complex and observed that the major species formed under catalytic conditions was probably a hydrido ethoxy complex. In order to facilitate a more detailed mechanistic understanding, complex **1** was investigated by a series of stoichiometric reactions.

Treatment of **1** with one or more (up to 10) equivalents of a ketone or an aldehyde in an aprotic solvent (benzene, toluene or acetone) results in minor conversion (approx. 10%) to two complexes that gave rise to two equally sized singlet resonances in the ^{31}P{^{1}H} NMR spectrum. One singlet is assignable to the *trans*-dihydride **4a** (Scheme 2) indicating that

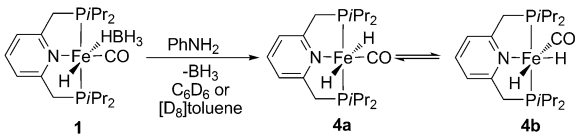

Scheme 2. Reaction of **1** with aniline.

in aprotic solvents, **1** preferably undergoes elimination of BH_3. Upon treatment of **1** with aniline (instead of a ketone or an aldehyde) as a BH_3 acceptor in benzene or toluene, complete reaction was observed to give two products with singlet resonances at $\delta = 116.86$ and 120.06 ppm in the

Table 2. Hydrogenation of ketones catalyzed by **1**.[a]

Entry[a]	Substrate	Product[b]	Yield [%] (Conversion)[b]	TON	TOF [h^{-1}]
	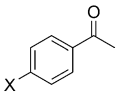	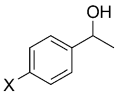			
1	X = H		89 (89)	1780	296
2[c]	X = H		99 (99)	1485	247
3	X = Cl		72 (72)	1440	240
4	X = Br		56 (60)	1120	186
5	X = Me		53 (53)	1060	176
6			44 (44)	880	146
7	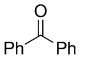		72 (72)	1440	240
8	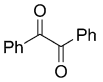	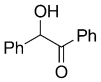	18	360	60
9			99 (99)	1980	330
10[d]	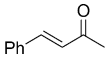	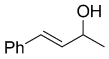	27 (99)	990	165
		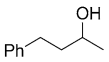	65		
		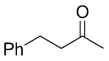	7		
11[e]			15 (15)	300	50

[a] Reaction conditions: **1** (0.0025 mmol), substrate (5 mmol), *m*-xylene (1 mmol) ethanol (3 mL), H_2 (4.1 atm), 40 °C, 6 h. [b] Determined by GC analysis with *m*-xylene as internal standard. [c] 0.0033 mmol of **1**. [d] 2.5 mmol of substrate. [e] 0.04 mmol KO*t*Bu were added.

$^{31}P\{^1H\}$ NMR spectrum (Scheme 2). The ^1H NMR spectrum of the mixture at room temperature exhibited a triplet at $\delta = -7.27$ ppm for the *trans*-dihydride **4a**, while no signal in the hydride region was observed for the second complex **4b** (by ^1H,^{31}P-HMQC NMR). Two complete sets of signals were observed for the hydrogen atoms of the pincer ligands: one set corresponding to the *trans*-dihydride **4a**, exhibiting only one signal for the methyl protons of the isopropyl groups and one signal for the benzylic protons, as expected for C_2, C_s or C_{2v} symmetry, and a second set for complex **4b** comprising four signals for the methyl protons of the isopropyl groups, indicating lack of symmetry (confirmed by ^1H-COSY, ^1H,^{13}C-HSQC NMR). At −70 °C, two triplets of doublets localized at $\delta = -18.65$ and −6.43 ppm were observed in the hydride region of the ^1H NMR spectrum, which are identified with **4b**. These findings, along with the J(H,H) value of 13.7 Hz, are consistent with **4b** being an iron(II) *cis*-dihydride complex.[18] In contrast to the observations at low temperature, only one broad singlet resonance at $\delta = -12.95$ ppm was observed at 90 °C for the two hydrides of **4b**, while the signals were absent at room temperature. Variable temperature ^1H-NOESY NMR experiments showed exchange between both hydride signals of **4b** and no exchange between **4a** and **4b** at −70 °C, while at 90 °C, exchange was observed between **4a** and **4b** (Scheme 2). The T_1(min) values measured at 500 MHz of 246 (**4b**) and 296 (**4a**) ms are in the range between classical and non-classical metal hydrides,[18] but the fact that **4a** and **4b** undergo H/D exchange in the presence of D_2 without any deuteration of the benzylic positions of the coordinated ligand suggests a mechanism involving a non-classical dihydrogen iron(0) intermediate. Complexes **4a** and **4b** did not show any significant reactivity towards acetophenone (after one day), indicating that they are not active species in the catalytic reduction of ketones.

When complex **1** was dissolved in CD_3OD, two additional complexes were observed in the ^1H and $^{31}P\{^1H\}$ NMR spectra in low concentrations relative to **1** (Scheme 3).[16] The

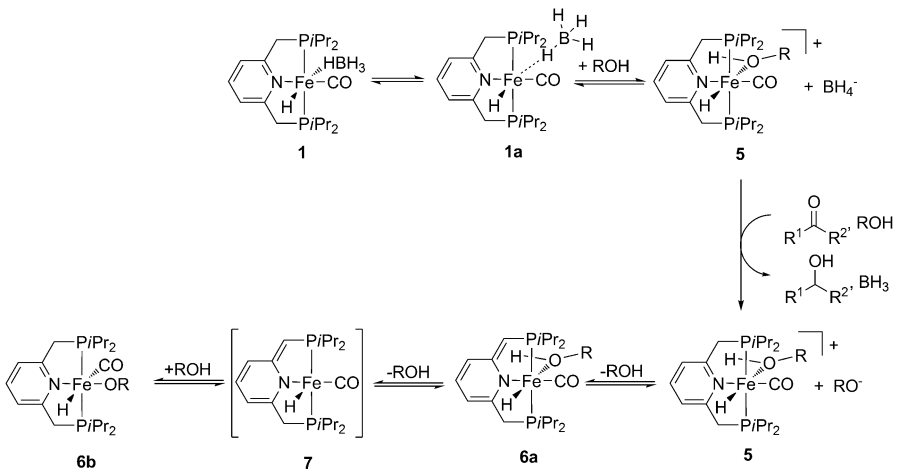

Scheme 3. Reactivity of **1** with ketones in alcohols (R = Me, Et).

first complex **1a** exhibits a broad singlet at $\delta = -5.71$ ppm in the ^{1}H NMR spectrum for the still coordinated tetrahydridoborate ligand and a triplet resonance at $\delta = -18.39$ ppm for the hydride ligand, which correlates to a signal at $\delta =$ 89.58 ppm in the ^{31}P{^{1}H} NMR spectrum. In comparison to **1**, the ^{1}H NMR signals of the hydride and the tetrahydridoborate ligand and the whole set of signals arising from the pincer ligand in **1a** are slightly shifted. The upfield shift of the hydride ligand in the ^{1}H NMR indicates a weaker association of the coordinated tetrahydridoborate ligand *trans* to it, and the appearance of a broad singlet instead of a broad doublet in the ^{1}H NMR might indicate a lower barrier of rotation for the tetrahydridoborate ligand in **1a**, which is in agreement with a weaker association.[20] The bonding in transition-metal borohydride complexes is usually described as a 2-electron 3-center bond; for the η^1-case, one of the t_2 orbitals of the borohydride ligand interacts with an appropriate orbital of the transition metal fragment.[21] A reasonable explanation for the observation made with complex **1a** could be that the bond between the iron(II) center and the borohydride ligand is less covalent together with a possible solvation effect of the borohydride ligand.

The second complex was identified as the cationic hydrido carbonyl complex $[(i\text{Pr-PNP})\text{Fe(CO)(H)(DOCD}_3)]^+$ (**5**-CD_3OD), which can also be independently prepared from **3** and $TlPF_6$ in CD_3OD. If one or two equivalents of acetophenone or benzaldehyde are added to this mixture, the concentrations of **1a** and **5**-CD_3OD increase immediately. ^{1}H-NOESY NMR experiments show an exchange between the hydride resonances of **1** and **1a** and between the hydride resonances of **1a** and **5**-CD_3OD. Formation of a cationic ruthenium species with an alcoholic solvent coordinated to the metal center was reported for hydrido borohydride ruthenium complexes.[10b,22] The observation of a cationic complex indicates that the tetrahydridoborate ligand dissociates prior to the aldehyde or ketone reduction to the corresponding alkoxides. A stoichiometric amount of base can be generated by alcoholysis of free borohydride as observed by Noyori and co-workers for the corresponding ruthenium hydrido borohydride complexes *trans*-[(tolbinap)-(diamine)RuH(η^1-BH_4)] (tolbinap = 2,2′-bis(di-4-tolylphosphino)-1,1′-binaphthyl; diamine = e.g., 1,2-diphenylethylenediamine) or reduction of acetophenone by the free borohydride anion.[10b,22] After 2–3 h of reaction with acetophenone or benzaldehyde, a new species (**6b**-CD_3OD) with a triplet resonance for the hydride ligand centered at $\delta =$ -6.39 ppm ($^2J_{PH} = 44.9$ Hz) in the ^{1}H NMR spectrum and a singlet peak at $\delta = 98.98$ ppm in the ^{31}P{^{1}H} NMR spectrum was observed.[20] The ^{1}H NMR chemical shift of $\delta =$ -6.39 ppm indicates that a strong donor is located *trans* to the hydride, likely the CO ligand. The fact that **6b**-CD_3OD is observed in reactions with benzaldehyde and acetophenone suggests that these are not bound to the iron(II) center in **6b**-CD_3OD. In fact, it seems likely that an alkoxide ligand is bound to the iron center.

When the reactions described above were conducted with benzaldehyde or acetophenone in [D_6]ethanol instead of [D_4]methanol, **1a** and the corresponding ethanol complex **5**-CD_3CD_2OD were initially formed, but the concentration of **5**-CD_3CD_2OD was significantly lower than in the corresponding reactions with [D_4]methanol. In addition to **6b**-CD_3CD_2OD, a new hydridic species with a doublet of doublet resonance at $\delta = -22.97$ ppm in the ^{1}H NMR ($^2J(H,P) =$ 61.3, $^2J(H,P) = 47.2$ Hz) and an AB-system centered at $\delta =$ 116.42 ppm in the ^{31}P{^{1}H} NMR spectrum ($^2J_{PP} = 143.6$ Hz) was generated over the course of the reaction (**6a**-CD_3CD_2OD). The observation of an AB system in the ^{31}P{^{1}H} NMR spectrum and a doublet of doublets for the hydride ligand in the ^{1}H NMR spectrum is consistent with a dearomatized complex with two inequivalent phosphorus centers. Based on the chemical shift of the hydride ligand and the observation of this complex in reactions with benzaldehyde and acetophenone, it seems likely that this complex is the dearomatized hydrido carbonyl ethanol iron(II) complex **6a**-CD_3CD_2OD. An unsaturated pentacoordinated intermediate **7** could be generated from **6a**-CD_3CD_2OD by the loss of the coordinated CD_3CD_2OD (Scheme 3).

Based on these observations, the reaction mechanism for the reduction of ketones by (*i*Pr-PNP*)Fe(H)(CO) (**7**, Figure 3, the asterisk denotes a dearomatized pincer ligand)[8] was examined using density functional theory (DFT), specifically at the SMD(EtOH)-PBE0-d_{v3}/cc-pVDZ//DF-PBE-d_{v2}/SDD(d) level of theory (see Computational Details section for full details). In particular, the reduction of acetophenone to 1-phenylethanol was considered, which involves an overall reaction energy of $\Delta G_{298} =$ -6.4 kcal mol^{-1}.

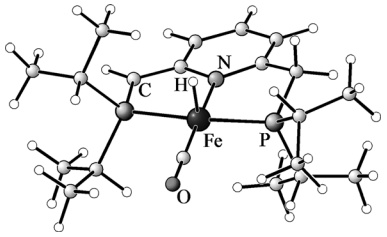

Figure 3. Optimized structure of **7** (a color version is provided in the Supporting Information).

One key constraint to be considered when evaluating possible reaction pathways involves the coordination site of the ketone (and its derivatives). The ketone has significant bulk and one would expect it to remain in the equatorial plane (as defined by the pincer ligand). If the ketone were to be in an axial/apical coordination site, one might expect significant steric interactions between it and the bulky isopropyl substituents.[23] The hydride and CO ligands are much smaller and thus more suitable ligands to occupy these sterically hindered sites.

The first proposed mechanism (Scheme 4, the determined reaction profile is in Figure 4 and the relative energies are in Table 3) is based on what one would intuitively draw based on the catalyst structure and is, in part, based on the mechanism proposed in the original communication.[8] The

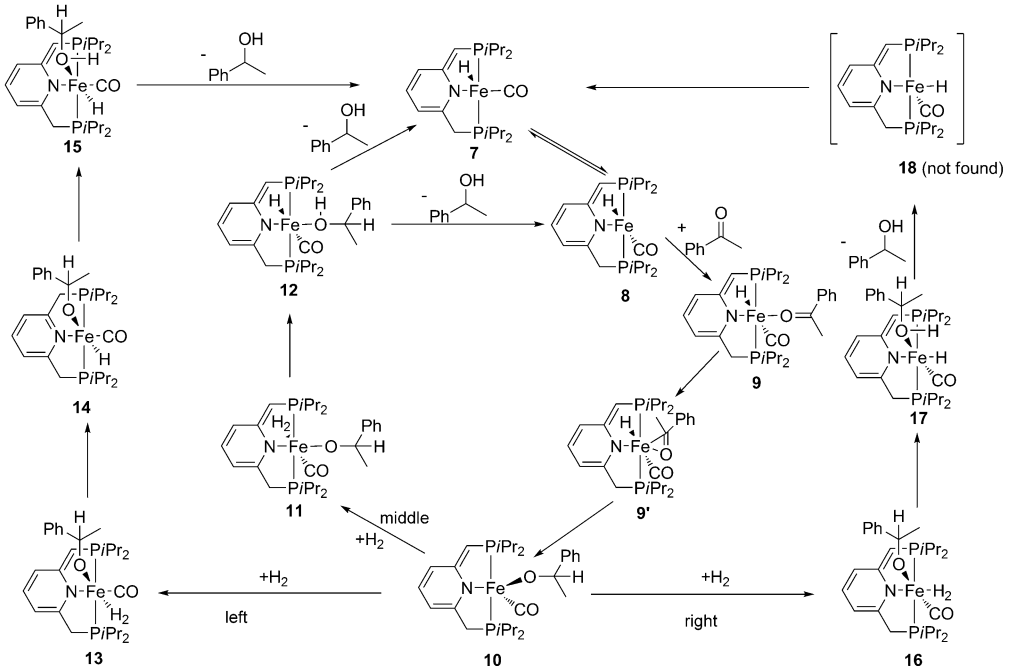

Scheme 4. Reaction mechanism for the [(*i*Pr-PNP*)Fe(H)(CO)] (**7**) catalyzed hydrogenation of acetophenone via initial iron hydride transfer to the acetophenone carbonyl carbon; the three possible pathways of the H_2 activation by **10** are indicated.

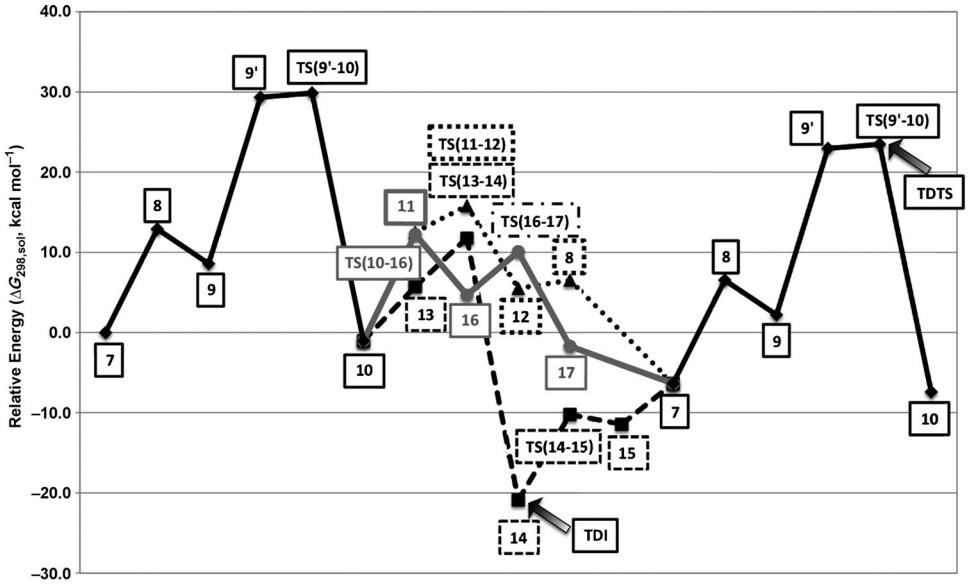

Figure 4. Reaction profile for the [(*i*Pr-PNP*)Fe(H)(CO)] (**7**) catalyzed hydrogenation of acetophenone via initial iron hydride transfer to the acetophenone carbonyl carbon (see Scheme 4). Only the routes involving the "**a**" isomers are shown; the "**b**" isomers are generally close in energy to their "**a**" counterparts. Parts common to all three pathways are drawn as solid lines, while the top, side and bottom approaches of H_2 are drawn as dotted, grey and dashed lines, respectively. Also shown are the turnover frequency (TOF) determining intermediate (TDI) and TOF determining transition state (TDTS) according to the energetic span model (ESM, see text) for this reaction profile.

first step involves isomerization of **7** to give the isomer **8** with the ring in the apical position, rather than the hydride. This is not as unfavourable as one might expect, as the nitrogen is an amide (R_2N^-) rather than a pyridine due to dearomatization of the PNP ligand. This allows for coordination of acetophenone to the equatorial coordination site (**9**) *cis* to the hydride. If the acetophenone were to coordinate to the vacant axial position in **7**, the hydride has to be transferred to the other face of the complex. In Ir and Ru complexes, this was found to be possible via the dearomatized ligand arm, but this transfer involves significant barriers, although solvent can facilitate this process.[23,24] In Ir^I, this transfer, when assisted by two water molecules, involves a calculated barrier of $\Delta G^{\ddagger}_{298} = 19.8\ kcal\,mol^{-1}$,[23a] higher than the isomerization energy **7**→**8** of $\Delta G^{\ddagger}_{298} = 12.9\ kcal\,mol^{-1}$. Nonetheless, such a pathway was also considered (see below).

Four acetophenone complexes were considered: two possible relative orientations of the acetophenone and CO ligands (in the Supporting Information and Table 3, these are identified by "a" and "b"; herein only the more stable will be considered although generally both are of similar energy—in a few cases only one of the isomers could be found), and two possible coordination

Table 3. DFT energies (kcal mol^{-1}, SMD(EtOH)-PBE0-d_{v3}/cc-pVDZ//DF-PBE-d_{v2}/SDD(d) level of theory) of all calculated structures, relative to **7**+acetophenone+H_2. Note that some of the complexes are only referred to in the expanded discussion in the Supporting Information (see text).

Complex		a	b	Complex		a	b
7	0.0			**22**		7.2	10.2
8	12.9			TS(**7–21**)	35.7		
9		8.6	11.7	TS(**7–21**)+EtOH	20.6		
9′		29.3	28.7	TS(**7–21**)+H_2O	23.9		
TS(**9–10**)		32.1	–[a]	**21**	7.4		
TS(**9′–10**)		29.9	–[a]	TS(**22–10**)		28.8	33.3
TS(**9–10**)+EtOH		63.4	–[a]	TS(**25–28**)		33.7	40.9
10		−1.0	0.0	**28**		−5.0	−9.7
11		12.5	7.8	TS(**28–11**)		21.3	16.0
TS(**11–12**)		15.8	13.4	TS(**28–30**)		29.0	23.3
12		5.5	4.0	**30**		2.9	6.7
13		5.7	2.8	TS(**26–29**)		36.0	27.3
TS(**13–14**)		11.8	9.5	**29**		−17.4	−18.5
14		−20.9	−21.9	TS(**29–30**)		11.9	13.2
TS(**14–15**)		−10.2	−10.4	TS(**23–24**)		26.2	30.1
15		−11.4	−12.7	**38**	7.6		
TS(**10–16**)		12.2	–[a]	TS(**38–32**)		24.5	21.7
16		4.7	3.5	**32**		−4.0	−1.7
TS(16–17)		10.1	10.3	**33**	−0.5		
17		−1.7	−2.0	**34**	6.3		
TS(**9–19**)		59.5	58.9	TS(**34–35**)	13.1		
19		15.6	16.6	**35**	−2.6		
19′		31.4	26.3	**36**	2.1		
20		1.3	−0.4	TS(**36–37**)	10.6		
TS(**20–22**)		34.1	33.4	**37**	−6.4		

[a] Not found; see text.

modes η^1-O and η^2-CO (denoted by no prime and prime, respectively)—of the ketone. While the two relative isomers of **9** are of similar energy (**9a** and **9b** differ by 3.1 kcal mol^{-1}, while **9a′** and **9b′** differ by 0.6 kcal mol^{-1}), the η^1-O isomers are significantly lower in energy.

The next step is the transfer of the metal hydride to the carbonyl carbon (**10**); previous work has shown the preference of hydrogen transfer to the carbonyl carbon over the carbonyl oxygen in the initial step in metal-catalyzed hydrogenation of acetone.[25] While **9** is lower in energy than **9′**, the transition state TS(**9–10**) results in a higher barrier than TS(**9′–10**) (Figure 5). The preferred route would thus involve changing binding modes of the acetophenone followed by a very low barrier (<1 kcal mol^{-1}) for hydrogen transfer. This transition state is the highest point on the reaction profile at $\Delta G^{\ddagger}_{298}$=29.9 kcal mol^{-1} relative to **7**+ reactants. Attempting to use a solvent (ethanol) molecule to lower this barrier by acting as a proton shuttle (see below) actually leads to a much higher barrier (i.e., TS(**9–10**)+EtOH, Table 3).

The next logical step is coordination of free H_2 to the vacated coordination site. As complex **10** is roughly trigonal bipyramidal, there are three possibilities for the H_2 to approach the metal center. One approach, the middle approach, relative to the PNP plane (Scheme 4), places the non-classical dihydrogen ligand *cis* to an equatorial 1-phenylethoxy ligand and thus well located to complete the hydrogenation. In fact, the barrier resulting from TS(**11–12**) (Figure 5) to give the 1-phenylethanol product complex **12** is fairly low ($\Delta G^{\ddagger}_{298}$=3.3 kcal mol^{-1}). Loss of the product alcohol from **12** regenerates the catalyst (**7** or **8**).

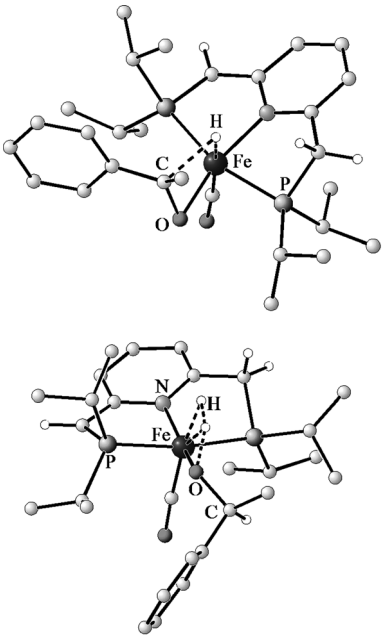

Figure 5. Optimized structures of TS(**9′–10**) (top) and TS(**11–12**) (bottom). For visual clarity, only the relevant hydrogen atoms are represented (a colour version is provided in the Supporting Information).

The second (left) approach (Scheme 4) of H_2 to complex **10** results in a complex with the H_2 ligand *trans* to the axial 1-phenylethoxy ligand **13**. This places this large ligand amongst the phosphine isopropyl substituents. Despite previous expectations, this complex is actually more stable than

its expected isomer **11** by 6.8 kcal mol^{-1}. In contrast to the first route, the H_2 is on the wrong side of the complex for direct transfer to the 1-phenylethoxy ligand. However, in related complexes it has been shown that the arm of the dearomatized pincer ligand can accept a hydrogen atom and thus be used as a shuttle between the two faces of the pincer ligand.[23,24,26] The barrier for hydrogen transfer (Figure 6, $\Delta G^{\ddagger}_{298} = 6.1$ kcal mol^{-1} from **13** to give **14**) from

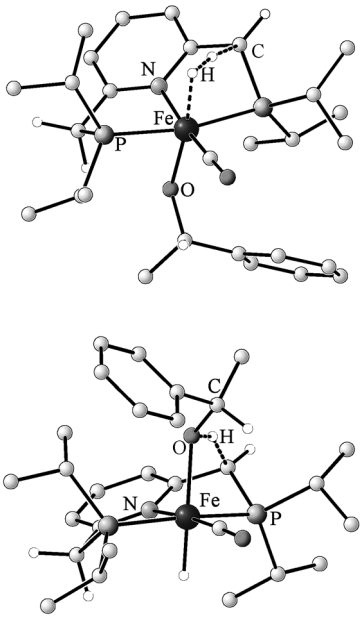

Figure 6. Optimized structures of TS(**13**–**14**) (top) and TS(**14**–**15**) (bottom). For visual clarity, only the relevant hydrogen atoms are represented (a colour version is provided in the Supporting Information).

the H_2 ligand to the arm is not unreasonable and is, in fact, dramatically lower than in the previously examined iridium complex.[23a] Complex **14** represents the lowest energy point on the reaction profile at $\Delta G_{298} = -19.3$ kcal mol^{-1}. Transfer of a hydrogen atom from the arm directly to the 1-phenylethoxy ligand (i.e., TS(**14**–**15**), Figure 6) generates the 1-phenylethanol product and regenerates the catalyst **1**. This involves a barrier of $\Delta G^{\ddagger}_{298} = 10.7$ kcal mol^{-1}.

A third (right) approach (Scheme 4) has the H_2 approaching between the CO and 1-phenylethoxy ligand, resulting in complex **16**. From **16**, a transition state for H_2 coordination TS(**10**–**16**) (Figure 7) was found, leading to a barrier of $\Delta G^{\ddagger}_{298} = 13.3$ kcal mol^{-1}, but its connectivity could not be confirmed by an IRC calculation. However, this point is still below TS(**9**–**10**) and thus should not significantly affect the reaction kinetics. From here, a low barrier (i.e., TS(**16**–**17**), Figure 7) leads to the coordinated alcohol complex **17** and finally regeneration of the catalyst.

All three approaches have similar barriers. However, the second approach involves a low energy intermediate **14**. This would result in a very slow reaction as the energy required to overcome TS(**9**–**10**) from this well is nearly 50 kcal mol^{-1}. Because of this high barrier (turnover frequency

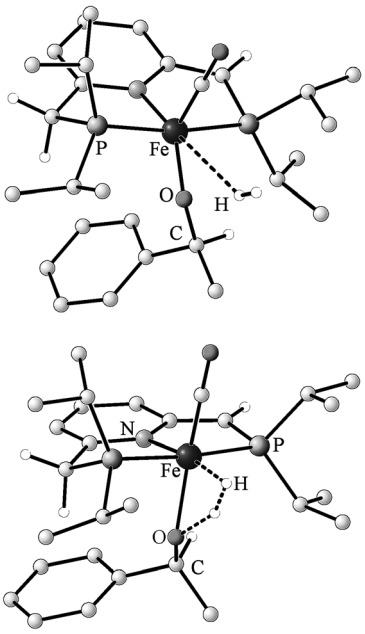

Figure 7. Optimized structures of TS(**10**–**16**) (top) and TS(**16**–**17**) (bottom). For visual clarity, only the relevant hydrogen atoms are represented (a colour version is provided in the Supporting Information).

(TOF)-determining transition state TDTS),[27] alternate routes that bypass either point, or both, were considered.

Several alternate pathways were considered before the final pathway was determined; the interested reader is referred to the Supporting Information for a brief discussion. The final, proposed reaction pathway (Scheme 5 and Figure 8) involves initial aromatization of **7** to give **21**. This transformation, which is assisted by a solvent (ethanol) molecule, involves a barrier TS(**7**–**21**)+EtOH of $\Delta G^{\ddagger}_{298} =$ 20.6 kcal mol^{-1}. This ethanol (or another) can coordinate to the metal center to give **38**. Next, a transition state was found for the concerted, dual hydrogen transfer of a hydrogen from the PNP-arm to the incoming acetophenone carbon and, in addition, the proton from the coordinated ethanol to the oxygen of the acetophenone ligand (i.e., to give complex **32**). An intrinsic reaction coordinate (IRC, see Computational Details section) calculation demonstrates that this transition state TS(**38**–**32**) (Figure 9) connects complex **38** and free acetophenone with complex **32**. This dual hydrogen transfer involves a barrier of $\Delta G^{\ddagger}_{298} = 24.5$ (**a**) or 21.7 (**b**) kcal mol^{-1}, relative to **7**+ reactants. Moreover, the low-energy structure **14** is avoided. Loss of 1-phenylethanol gives the iron-ethoxide complex **33**, which upon addition of H_2, regenerates the catalyst. Catalyst regeneration can either proceed via TS(**34**–**35**) or TS(**36**–**37**) (Scheme 5 and Figure 8), which differ in approach of H_2 (i.e., side or bottom) involve barriers of $\Delta G^{\ddagger}_{298} = 13.1$ or 10.6 kcal mol^{-1} (relative to **7**+reactants). As both routes for catalyst regeneration involve low barriers, both are feasible and likely to occur. According to the energetic span model (ESM),[27] the dual hydrogen transfer transition state TS(**38**–**32**) is the TDTS, while the initial reactants +**7** form the TOF-deter-

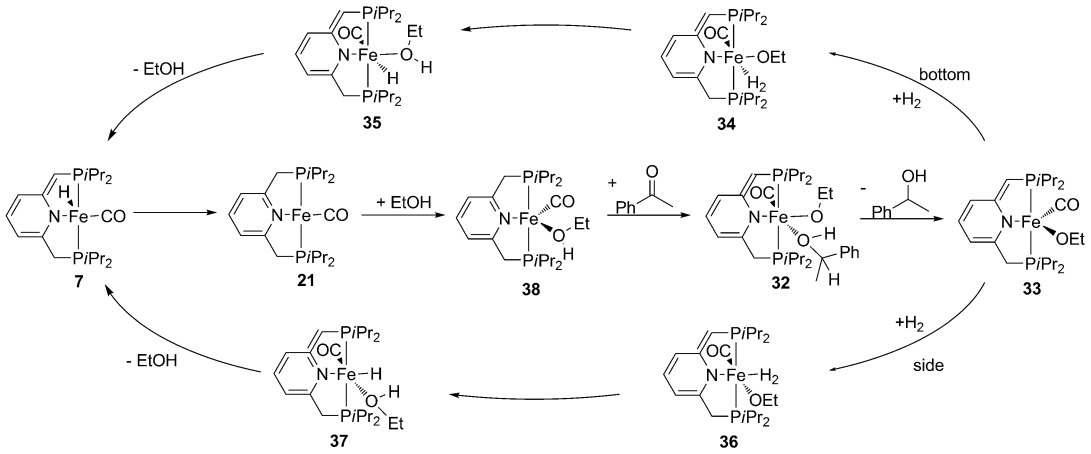

Scheme 5. Final reaction mechanism found for the [(*i*Pr-PNP*)Fe(H)(CO)] catalyzed hydrogenation of acetophenone. Catalyst regeneration can proceed via either side or bottom approach (as indicated) of H_2 to **33**, both of which are feasible.

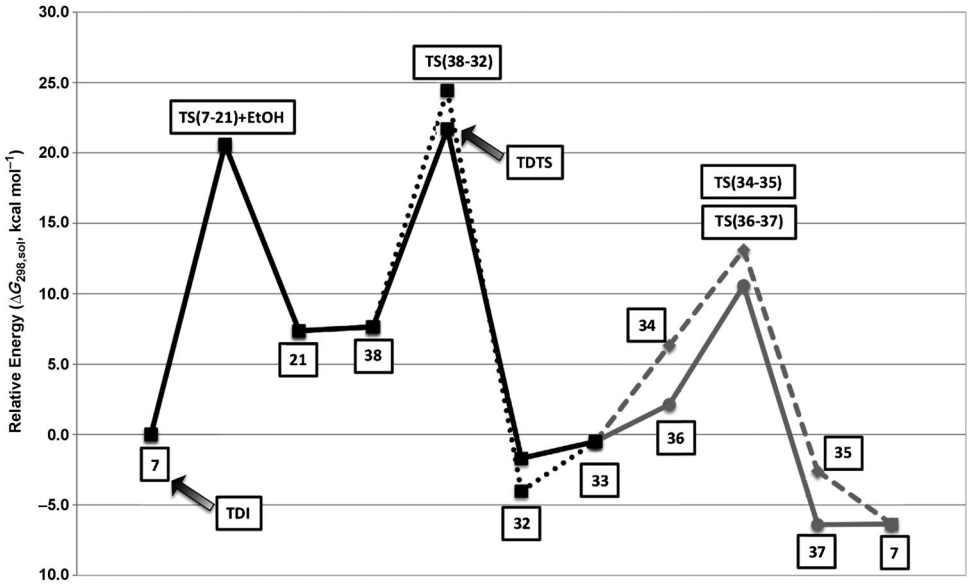

Figure 8. Reaction profile for the (*i*Pr-PNP*)Fe(H)(CO) catalyzed hydrogenation of acetophenone via the final reaction pathway. The exit routes via **34** and **36** ar drawn as dashed and solid grey lines, respectively, both of which are feasible. The lower-energy "**b**" route is shown in solid lines while the alternate "**a**" route, which differs in the orientation of the acetophenone as it approaches the metal center, is in dotted lines, and both routes are feasible (see text). Also shown are the TDI and TDTS according to the ESM (see text) for this reaction profile.

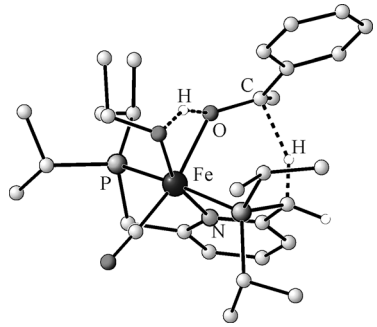

Figure 9. Optimized structures of TS(**38**–**32**). For visual clarity, only the relevant hydrogen atoms are shown (a color version is provided in the Supporting Information).

mining intermediate (TDI), which results in a very reasonable energetic span of $\Delta G^{\ddagger}_{298} =$ 24.5 (**a**) or 21.7 (**b**) kcal mol^{-1}. Both of these values are reasonable for a room temperature reaction. The two transition states only differ in the orientation of the acetophenone (namely vis-á-vis the Fe–CO axis) during its approach to the metal center. Thus the reaction can occur regardless of the approach and the ketone need not reorient itself, which would slow down the catalysis.

Yang recently reported an independent computational study into the mechanism of the (*i*Pr-PNP*)Fe(H)(CO) catalyzed reduction of acetophenone.[41] In their mechanism, the reaction proceeds via *trans*-(*i*Pr-PNP)Fe(H)$_2$(CO) and involves an outer-sphere hydrogen-transfer from this complex to the carbonylcarbon atom of acetophenone to yield, as an intermediate, 1-phenylethoxide, which binds to the metal center and subsequently a hydrogen atom is transferred from the arm. We have certain reservations about this mechanism and favor ours for a few reasons: a) Yang's mechanism goes via *trans*-(*i*Pr-PNP)Fe(H)$_2$(CO). However, we demonstrate here that the dihydride complexes **4a** and **4b** do not reduce acetophenone (see above). b) Yang's study used methyl substituents on the PNP ligand rather than isopropyl. While this was shown in two cases not to have an impact on the results, this may not be so throughout the reaction, and especially in the key transition state (denoted by Yang as $TS_{7,11}$) involving hydro-

gen-transfer to the acetophenone carbonyl carbon. This transition state requires a precise alignment of the complex and the substrate in the outer sphere and steric interactions might be significant. At the very least, steric influence cannot be summarily dismissed based on their insignificance in another transition state along the reaction profile. This was demonstrated in our previous examination of the *trans*-addition of H_2 to (*t*Bu-PNP)IrPh.[23a] Sterics may also affect another key transition state $TS_{2,9\text{-EtOH}}$ in Yang's mechanism, specifically protonation of the PNP* arm C=C bond by ethanol. c) Yang's mechanism involves a very specific approach of acetophenone to the iron center without any directing influences. By analogy, in heterogeneous catalysis the Langmuir–Hinshelwood (LH) mechanism[42] is generally favored over the Eley–Rideal (ER) mechanism,[43] even though the latter tends to have lower reaction barriers.[44] This is explained in part by noting that the channel for the incoming substrate is narrow and any small deviations can result in significantly higher barriers.[44] In contrast, in our mechanism, the incoming acetophenone substrate is directed to the metal center by the Fe–O interaction and both approaches of the substrate can lead to a viable reaction. A related metal–oxygen directing interaction has demonstrated experimentally in the ruthenium-based Noyori reduction of acetophenone.[45]

Conclusion

In summary, we have described the synthesis and characterisation of two rare examples of stable mononuclear iron(II) hydrido borohydride complexes. The hydrido carbonyl tetrahydridoborate complex **1** catalyzes the hydrogenation of ketones under mild conditions with no added base, with turnover numbers of up to 1980, which is the highest turnover number reported to date for iron-catalyzed hydrogenation. The *cis*- and *trans*-dihydride carbonyl complexes **4a** and **4b**, which are in equilibrium with one another, do not react with acetophenone, excluding the possibility that these complexes are the active species in the catalytic reduction of ketones. Furthermore, the reaction mechanism of the iron-catalyzed hydrogenation of ketones was examined using density functional theory. It was found that the preferred route involves the following steps: i) alcohol-assisted aromatization of **7** to give initially **21** and subsequently ethanol coordination to give **38**; ii) concerted coordination of acetophenone and dual hydrogen-atom transfer from the PNP arm and the coordinated ethanol to, respectively, the carbonyl carbon and oxygen atoms; iii) release of the 1-phenylethanol product and coordination of H_2; and iv) proton transfer to the alcohol and regeneration of the catalyst. This overall reaction pathway involves an overall barrier (energetic span according to the ESM) of $\Delta G^{\neq}_{298} = 21.7$ kcal mol^{-1}. Attempts to develop asymmetric variants of this reaction are in progress.

Experimental Section

Materials and methods: All experiments were carried out under an atmosphere of purified nitrogen in a Vacuum Atmospheres glovebox or using standard Schlenk techniques. All solvents were reagent grade or better. Benzene and *n*-pentane were refluxed over sodium/benzophenone and distilled under argon atmosphere. Ethanol and acetonitrile were cooled with liquid nitrogen and degassed under vacuum. Deuterated solvents were degassed with argon and stored in the glovebox. All substrates for hydrogenation were purified by either distillation or recrystallization. The *i*Pr-PNP ligand,[28] [(*i*Pr-PNP)Fe(CO)Br$_2$][8] and [(*i*Pr-PNP)Fe(H)(CO)Br][8] (**3**) were prepared according to previously reported procedures. ^{1}H, ^{13}C and ^{31}P NMR spectra were recorded using Bruker Avance III-300, Avance III-400 or Avance II-500 NMR spectrometers. ^{1}H and ^{13}C{^{1}H} and ^{13}C-DEPTQ NMR chemical shifts (δ) are reported in ppm downfield from tetramethylsilane and calibrated using the solvent peaks. ^{31}P NMR chemical shifts are reported in ppm downfield from H_3PO_4 and referenced to an external 85% solution of phosphoric acid in D_2O. IR spectra were recorded on a Nicolet FT-IR spectrophotometer. Mass spectra were recorded on a Micromass Platform LCZ 4000, in the Electro Spray Ionization (ESI) mode. Elemental analyses were performed on a Thermo Finnigan Italia S.p.A-FlashEA 1112 CHN Elemental Analyzer.

General Procedure for catalytic hydrogenation: A 90 mL Fischer–Porter tube was charged under nitrogen with catalyst **1** (0.0025 mmol), ethanol (3 mL), ketone (5 mmol) and *m*-xylene (1 mmol). The nitrogen present in the tube was replaced by hydrogen and the tube was pressurized with hydrogen (4.1 atm). The solution was stirred at 40 °C for the specified time (Table 2) and the extent of conversion to the corresponding alcohols was determined by GC analysis with *m*-xylene as internal standard, using a Carboxen 1000 column on a HP 690 series GC system.

[(*i*Pr-PNP)FeH(CO)(BH$_4$)] (1): [(*i*Pr-PNP)Fe(CO)Br$_2$] (194.9 mg, 0.334 mmol) was suspended in EtOH (12 mL) and $NaBH_4$ (66.0 mg, 1.745 mmol, 5.2 equiv) was added in one portion. After stirring at ambient temperature for 3 h, a red solution was obtained. The solvent was removed in vacuo, C_6H_6 (10 mL) was added and the mixture was filtered through Celite. The filtrate was concentrated in vacuo and the resulting reddish-brown residue was washed with pentane to give a yellow solid (102.8 mg, 70%). ^{1}H NMR (300 MHz, C_6D_6, 25 °C): $\delta = 6.66$ (t, ^3J(H,H) = 7.6 Hz, 1H, pyrdine-H_4), 6.38 (d, ^3J(H,H) = 7.6 Hz, 2H, pyridine-$H_{3,5}$), 3.62 (dvt, ^2J(H,H) = 13.2 Hz, ^3J(H,P) = 3.2 Hz, 2H, C*H*HP*i*Pr$_2$), 2.92–2.74 (m, 2H+2H, overlapped PC*H*(CH$_3$)$_2$ and CH*H*P*i*Pr$_2$), 2.05–1.90 (m, 2H, PC*H*(CH$_3$)$_2$), 1.49 (dd, ^3J(H,P) = 15.4 Hz, ^3J(H,H) = 7.3 Hz, 6H, PCH(C*H*$_3$)$_2$), 1.23 (dd, ^3J(H,P) = 12.8 Hz, ^3J(H,H) = 7.2 Hz, 6H, PCH(C*H*$_3$)$_2$), 1.17 (dd, ^3J(H,P) = 15.6 Hz, ^3J(H,H) = 7.1 Hz, 6H, PCH(C*H*$_3$)$_2$), 0.76 (dd, ^3J(H,P) = 13.8 Hz, ^3J(H,H) = 6.7 Hz, 6H, PCH(C*H*$_3$)$_2$), −2.29 (br, 4H, Fe-*H*B*H*$_3$), −16.62 ppm (t, ^2J(H,P) = 50.8 Hz, 1H, Fe-*H*); ^{31}P{^{1}H} NMR (161 MHz, C_6D_6, 25 °C): $\delta = 93.57$ ppm (s); ^{13}C{^{1}H} NMR (126 MHz, C_6D_6, 25 °C): $\delta = 222.7$ (dt, ^2J(C,P) = 26.0 Hz, ^2J(C,H) = 18.9 Hz, Fe-*C*O), 163.6 (vt, ^2J(C,P) = 7.2 Hz, pyridine-$C_{2,6}$), 134.9 (s, pyridine-C_4), 119.0 (vt, ^3J(C,P) = 5.1 Hz, pyridine-$C_{3,5}$), 40.2 (vt, ^1J(C,P) = 7.8 Hz, *C*H$_2$P*i*Pr$_2$), 28.2 (vt, ^1J(C,P) = 9.9 Hz, P*C*H(CH$_3$)$_2$), 25.2 (vt, ^1J(C,P) = 13.4 Hz, P*C*H(CH$_3$)$_2$), 25.1 (vt, ^1J(C,P) = 13.7 Hz, P*C*H(CH$_3$)$_2$), 20.0 (vt, ^2J(C,P) = 1.3 Hz, PCH(*C*H$_3$)$_2$), 19.2 (vt, ^2J(C,P) = 2.6 Hz, PCH(*C*H$_3$)$_2$), 18.5 (s, PCH(*C*H$_3$)$_2$), 18.43 ppm (s, PCH(*C*H$_3$)$_2$); ^{1}H NMR (400 MHz, CD_3OD, 25 °C): $\delta = 7.48$ (t, ^3J(H,H) = 7.9 Hz, 1H, pyridine-H_4), 7.23 (d, ^3J(H,H) = 7.9 Hz, 2H, pyridine-$H_{3,5}$), 3.74 (dvt, ^2J(H,H) = 16.6 Hz, ^2J(H,P) = 3.6 Hz, 2H, CH*H*P*i*Pr$_2$), 3.64 (dvt, ^2J(H,H) = 12.3 Hz, ^2J(H,P) = 4.8 Hz, 2H, C*H*HP*i*Pr$_2$), 2.78–2.64 (m, 2H, PC*H*(CH$_3$)$_2$), 2.52–2.38 (m, 2H, PC*H*(CH$_3$)$_2$), 1.45 (dd, ^3J(H,P) = 14.8 Hz, ^3J(H,H) = 7.1 Hz, 6H, PCH(C*H*$_3$)$_2$), 1.40 (dd, ^3J(H,P) = 12.7 Hz, ^3J(H,H) = 6.9 Hz, 6H, PCH(C*H*$_3$)$_2$), 1.21 (dd, ^3J(H,P) = 15.5 Hz, ^3J(H,H) = 6.9 Hz, 6H, PCH(C*H*$_3$)$_2$), 0.93 (dd, ^3J(H,P) = 13.9 H, ^3J(H,H) = 6.9 Hz, 6H, PCH(C*H*$_3$)$_2$), −3.19 (br, 4H, Fe-*H*B*H*$_3$), −17.63 ppm (t, ^2J(H,P) = 52.2 Hz, 1H, Fe-*H*); ^{31}P{^{1}H} NMR (161 MHz, CD_3OD, 25 °C): $\delta = 94.57$ ppm (s); ^{1}H NMR (400 MHz, [D$_6$]ethanol, 25 °C): $\delta = 7.47$ (t, ^3J(H,H) = 7.6 Hz, 1H, pyridine-H_4), 7.24 (d, ^3J(H,H) = 7.6 Hz, 2H, pyridine-$H_{3,5}$), 3.65–3.48 (superimposed by residual solvent peak, 4H, CH*H*P*i*Pr$_2$ and C*H*HP*i*Pr$_2$), 2.82–2.66 (m, 2H, PC*H*(CH$_3$)$_2$),

2.50–2.38 (m, 2H, PC*H*(CH_3)$_2$), 1.46 (dd, ^3J(H,P) = 15.3 Hz, ^3J(H,H) = 7.82 Hz, 6H, PCH(C*H*$_3$)$_2$), 1.40 (dd, ^3J(H,P) = 13.1 Hz, ^3J(H,H) = 7.5 Hz, 6H, PCH(C*H*$_3$)$_2$), 1.22 (dd, ^3J(H,P) = 15.9 Hz, ^3J(H,H) = 7.3 Hz, 6H, PCH(C*H*$_3$)$_2$), 0.95 (dd, ^3J(H,P) = 13.4 Hz, ^3J(H,H) = 6.7 Hz, 6H, PCH(C*H*$_3$)$_2$), −3.14 (br, 4H, Fe-*H*B*H*$_3$), −17.48 ppm (t, 1H, ^2J(P,H) = 51.8 Hz, Fe-*H*); IR (thin film): $\tilde{\nu}$ = 2318 (m, ν_{BH}), 2269 (m, ν_{BH}), 2028 (br, ν_{BH}), 1916 (s, ν_{CO}), 1052 cm^{-1} (s, δ_{BH3}); ESI-MS (pos.): *m*/*z* (%): 424.13 (50) [M^+−BH_4]; elemental analysis calcd (%) for $C_{20}H_{40}BFeNOP_2$: C 54.70, H 9.18, N 3.19; found: C 54.27, H 9.14, N 3.26.

[(*i*Pr-PNP)FeH(BH$_4$)] (2): $FeBr_2$ (21.6 mg, 0.10 mmol) and *i*Pr-PNP (34.0 mg, 0.10 mmol) were dissolved in a mixture of MeCN (3 mL) and EtOH (3 mL), to give a pale red-orange solution. After 30 min, $NaBH_4$ (15.0 mg, 0.40 mmol) was added in one portion. Gas evolution took place and the color of the solution turned immediately to deep red. After 2 h of stirring at ambient temperature the solvent was removed in vacuo. Pentane (10 mL) was added to the residue, the mixture was filtered and the solvent of the resulting filtrate was removed in vacuo, to yield pure **2** as a dark red solid (34.3 mg, 83 %). ^{1}H NMR (400 MHz, C_6D_6, 25 °C): δ = 6.41 (t, ^3J(H,H) = 7.4 Hz, 1H, pyridine-*H*$_4$), 6.18 (d, 2H, ^3J(H,H) = 7.4 Hz, pyridine-*H*$_{3,5}$), 4.95 (br d, 2H, FeH_2BH_2), 3.07–2.85 (m, 4H + 2H, C*H*$_2$P*i*Pr$_2$ + PC*H*(CH_3)$_2$), 2.25–2.10 (m, 2H, PC*H*(CH_3)$_2$), 1.40–1.24 (m, 18H, PCH(C*H*$_3$)$_2$), 1.09 (dd, ^3J(H,P) = 13.1 Hz, ^3J(H,H) = 6.8 Hz, 6H, PCH(C*H*$_3$)$_2$), −9.63 (br, 1H, FeH*H*BH$_2$), −18.18 (t, ^2J(H,P) = 56.3 Hz, 1H, Fe-*H*), −28.67 ppm (br, 1H, Fe*H*HBH$_2$); ^{31}P{^{1}H} NMR (162 MHz, C_6D_6, 25 °C): δ = 97.68 ppm (s); ^{13}C{^{1}H} NMR (101 MHz, C_6D_6, 25 °C) δ = 167.1 (t, ^2J(C,P) = 6.6 Hz, pyridine-*C*$_{2,6}$), 129.3 (s, pyridine-*C*$_4$), 116.8 (t, ^3J(C,P) = 4.7 Hz, pyridine-*C*$_{3,5}$), 38.6 (t, ^1J(C,P) = 6.6 Hz, *C*H$_2$P*i*Pr$_2$), 24.4 (t, ^1J(C,P) = 11.3 Hz, P*C*H(CH$_3$)$_2$), 23.6 (t, ^1J(C,P) = 5.7 Hz, P*C*H(CH$_3$)$_2$), 19.3 (t, ^2J(C,P) = 3.4 Hz, PCH(*C*H$_3$)$_2$), 19.1 (s, PCH(*C*H$_3$)$_2$), 18.6 (s, PCH(*C*H$_3$)$_2$), 18.2 ppm (s, PCH(*C*H$_3$)$_2$); IR (thin film): $\tilde{\nu}$ = 2387 (s, ν_{BHt}), 2322 (s, ν_{BHt}), 1818 (br, ν_{BHb}), 1189 cm^{-1} (s, δ_{BH}); ESI-MS (*pos.*): *m*/*z* (%): 396.16 (100) [M^+−BH_4]; elemental analysis calcd (%) for $C_{19}H_{40}BFeNP_2$: C 55.51, H 9.81, N 3.41; found: C 54.89, H 9.74, N 3.42.

***trans*-[(*i*Pr-PNP)Fe(H)$_2$(CO)] (4a) and *cis*-[(*i*Pr-PNP)Fe(H)$_2$(CO)] (4b)**: [(*i*Pr-PNP)FeH(CO)(BH$_4$)] (**1**) (16.0 mg, 0.036 mmol) was dissolved in C_6D_6 or [D_8]toluene (0.5 mL) and $PhNH_2$ (3.4 mg, 0.036 mmol) was added. The reaction mixture was allowed to stand at ambient temperature for 5 d, during which the color of the solution became reddish-brown. The solution contained a mixture of two complexes in approximately 1:1 ratio, which were identified as *trans*-[(*i*Pr-PNP)Fe(H)$_2$(CO)] (**4a**) and *cis*-[(*i*Pr-PNP)Fe(H)$_2$(CO)] (**4b**). Both complexes are difficult to manipulate and undergo decomposition in vacuo. All attempts to precipitate or crystallize either complex from the reaction mixture were to no avail owing to their intrinsic solubility in common organic solvents. For this reason both complexes were characterized in solution by multinuclear NMR spectroscopy and assignments are based on ^{1}H,^{31}P-HMQC, ^{1}H-COSY, ^{1}H,^{13}C-HSQC and ^{1}H,^{13}C-HMBC NMR. The IR spectrum of the mixture measured as a thin film exhibits only one band for the CO vibration. IR (thin film): $\tilde{\nu}$ = 1870 cm^{-1} (CO).

NMR data for *trans*-[(*i*Pr-PNP)Fe(H)$_2$(CO)] (**4a**): ^{1}H NMR (400 MHz, C_6D_6, 25 °C): δ = 6.58 (t, ^3J(H,H) = 7.5 Hz, 1H, pyridine-*H*$_4$), 6.33 (d, ^3J(H,H) = 7.5 Hz, 2H, pyridine-*H*$_{3,5}$), 2.95 (br s, 4H, C*H*$_2$P*i*Pr$_2$), 2.17–2.04 (m, 4H, PC*H*(CH_3)$_2$), 1.40 (dd, ^3J(H,P) = 14.7 Hz, ^3J(H,H) = 7.0 Hz, 12H, PCH(C*H*$_3$)$_2$), 1.11 (dd, ^3J(H,P) = 12.9 Hz, ^3J(H,H) = 6.9 Hz, 12H, PCH(C*H*$_3$)$_2$), −7.27 ppm (t, ^2J(H,P) = 40.3 Hz, 2H, Fe-*H*); ^{31}P{^{1}H} NMR (162 MHz, C_6D_6, 25 °C): δ = 120.06 ppm (s); selectively decoupled ^{31}P{^{1}H} NMR (162 MHz, C_6D_6, 25 °C): δ = 120.07 ppm (t, ^2J(P,H) = 36.2 Hz); ^{13}C{^{1}H} NMR (101 MHz, C_6D_6, 25 °C): δ = 225.9 (t, ^2J(C,P) = 27.0 Hz, Fe-*C*O); 163.6 (vt, ^2J(C,P) = 6.2 Hz, pyridine-*C*$_{2,6}$), 132.0 (s, pyridine-*C*$_4$), 117.9 (vt, ^3J(C,P) = 4.8 Hz, pyridine-*C*$_{3,5}$), 39.2 (vt, ^1J(C,P) = 7.1 Hz, *C*H$_2$P*i*Pr$_2$), 26.6 (vt, ^1J(C,P) = 10.9 Hz, P*C*H(CH$_3$)$_2$), 19.2 (s, PCH(*C*H$_3$)$_2$), 18.2 ppm (s, PCH(*C*H$_3$)$_2$).

NMR data for *cis*-[(*i*Pr-PNP)Fe(H)$_2$(CO)] (**4b**): ^{1}H NMR (400 MHz, C_6D_6, 25 °C): δ = 6.64 (t, ^3J(H,H) = 7.5 Hz, 1H, pyridine-*H*$_4$), 6.42 (d, ^3J(H,H) = 7.5 Hz, 2H, pyridine-*H*$_{3,5}$), 3.06–2.87 (superimposed, 4H, C*H*$_2$P*i*Pr$_2$), 2.31–2.16 (m, 2H, PC*H*(CH_3)$_2$), 1.99–1.85 (m, 2H, P*C*H(CH$_3$)$_2$), 1.32 (dd, ^3J(H,P) = 14.1 Hz, ^3J(H,H) = 7.1 Hz, 6H, PCH(C*H*$_3$)$_2$), 1.29–1.18 (m, 12H, PCH(C*H*$_3$)$_2$), 0.96 ppm (dd, ^3J(H,P) = 13.6 Hz, ^3J(H,H) = 6.8 Hz, 6H, PCH(C*H*$_3$)$_2$); the two hydrogen atoms bound to the metal center are not observable at room temperature; ^{1}H NMR (500 MHz, [D_8]toluene, −60 °C): δ = −6.43 (td, ^2J(H,P) = 54.0 Hz, J(H,H) = 13.7 Hz, 1H, Fe(CO)H*H*), −18.65 ppm (td, ^2J(H,P) = 46.9 Hz, J(H,H) = 13.7 Hz, 1H, Fe(CO)*H*H); ^{1}H NMR (500 MHz, [D_8]toluene, 90 °C): δ = −12.95 ppm (br, 2H, Fe(CO)*HH*); ^{31}P{^{1}H} NMR (162 MHz, C_6D_6, 25 °C): δ = 116.86 ppm (s); ^{13}C{^{1}H} NMR (101 MHz, C_6D_6, 25 °C): δ = 223.0 (t, ^2J(C,P) = 14.9 Hz, Fe-*C*O), 162.6 (vt, ^2J(C,P) = 7.5 Hz, pyridine-*C*$_{2,6}$), 131.3 (s, pyridine-*C*$_4$), 117.7 (vt, ^3J(C,P) = 4.4 Hz, pyridine-*C*$_{3,5}$), 42.5 (vt, ^1J(C,P) = 6.6 Hz, *C*H$_2$P*i*Pr$_2$), 29.2 (vt, ^1J(C,P) = 9.1 Hz, P*C*H(CH$_3$)$_2$), 26.8 (vt, ^1J(C,P) = 12.8 Hz, P*C*H(CH$_3$)$_2$), 19.5 (br, PCH(*C*H$_3$)$_2$), 18.7 (s, PCH(*C*H$_3$)$_2$), 18.6 ppm (s, PCH(*C*H$_3$)$_2$).

[(*i*Pr-PNP)Fe(H)(CO)(DOCD$_3$)](PF$_6$) (5-CD$_3$OD): [(*i*Pr-PNP)Fe(H)(CO)Br] (20.0 mg, 0.04 mmol) and $TlPF_6$ (14.0 mg, 0.04 mmol) were suspended in CD_3OD (1 mL). A white precipitate of TlBr was formed immediately. After 30 min the mixture was filtered through a syringe filter to give an orange solution. The coordinated CD_3OD is labile and maybe removed from the iron center in vacuo or displaced by addition of other donor ligands. In addition, complex **5**-CD_3OD slowly decomposes in alcoholic solvents as described below. For this reason complex **5**-CD_3OD was characterized in solution by multinuclear NMR spectroscopy. ^{1}H NMR (500 MHz, CD_3OD, 25 °C): δ = 7.77 (t, ^3J(H,H) = 7.7 Hz, 1H, pyridine-*H*$_4$), 7.50 (d, ^3J(H,H) = 7.7 Hz, 2H, pyridine-*H*$_{3,5}$), 3.82 (dvt, ^2J(H,H) = 17.3 Hz, ^2J(H,P) = 5.0 Hz, 2H, CH*H*P*i*Pr$_2$), 3.71 (dvt, ^2J(H,H) = 17.3 Hz, ^2J(H,P) = 3.4 Hz, 2H, C*H*HP*i*Pr$_2$), 2.52–2.40 (m, 4H, PC*H*(CH_3)$_2$), 1.49 (dd, ^3J(H,P) = 14.1 Hz, ^3J(H,H) = 7.2 Hz, 6H, PCH(C*H*$_3$)$_2$), 1.43 (dd, ^3J(H,P) = 13.4 Hz, ^3J(H,H) = 7.1 Hz, 6H, PCH(C*H*$_3$)$_2$), 1.18 (dd, ^3J(H,P) = 15.9 Hz, ^3J(H,H) = 7.0 Hz, 6H, PCH(C*H*$_3$)$_2$), 0.88 (dd, ^3J(H,P) = 14.1 Hz, ^3J(H,H) = 6.9 Hz, 6H, PCH(C*H*$_3$)$_2$), −25.65 ppm (t, ^2J(H,P) = 54.2 Hz, 1H, Fe-*H*); ^{1}H{^{31}P} NMR (500 MHz, CD_3OD, 25 °C): δ = 7.80 (t, ^3J(H,H) = 7.7 Hz, 2H, pyridine-*H*$_4$), 7.53 (d, ^3J(H,H) = 7.7 Hz, 2H, pyridine-*H*$_{3,5}$), 3.85 (d, ^2J(H,H) = 17.6 Hz, 2H, CH*H*P*i*Pr$_2$), 3.73 (d, ^2J(H,H) = 17.6 Hz, 2H, C*H*HP*i*Pr$_2$), 2.54–2.42 (m, 4H, PC*H*(CH_3)$_2$), 1.52 (d, ^3J(H,H) = 7.3 Hz, 6H, PCH(C*H*$_3$)$_2$), 1.46 (d, ^3J(H,H) = 7.1 Hz, 6H, PCH(C*H*$_3$)$_2$), 1.20 (d, ^3J(H,H) = 6.9 Hz, 6H, PCH(C*H*$_3$)$_2$), 0.91 (d, ^3J(H,H) = 6.8 Hz, 6H, PCH(C*H*$_3$)$_2$), −25.62 ppm (s, 1H, Fe-*H*); ^{31}P{^{1}H} NMR (162 MHz, CD_3OD, 25 °C): δ = 88.13 (s, *P*-Fe-*P*), −141.44 ppm (sept, ^1J(P,F) = 707.7 Hz, *P*F$_6$); ESI-MS (pos., CH_3OH): *m*/*z* (%): 456.08 (5) [M^+], 452.15 (100) [{(*i*Pr-PNP)FeH(CO)$_2$}$^+$, decomp prod.], 378.15 (25) [{*i*Pr-PNP + K}$^+$, decomp prod.], 362.18 (30) [{*i*Pr-PNP + Na}$^+$, decomp prod.]; ESI-MS (neg., CH_3OH): *m*/*z* (%): 144.84 (100) [PF_6^-].

[(*i*Pr-PNP)Fe(H)(CO)(DOCD$_2$CD$_3$)](PF$_6$) (5-CD$_3$CD$_2$OD): [(*i*Pr-PNP)Fe(H)(CO)Br] (20.0 mg, 0.04 mmol) and $TlPF_6$ (14.0 mg, 0.04 mmol) were suspended in [D_6]ethanol (1 mL). A white precipitate of TlBr was formed immediately. After 30 min the mixture was filtered through a syringe filter to give an orange solution. Complex **5**-CD_3CD_2OD is less stable than **5**-CD_3OD and decomposes much faster. ^{1}H NMR (500 MHz, [D_6]ethanol, 25 °C): δ = 7.77 (d, ^3J(H,H) = 7.1 Hz, 2H, pyridine-*H*$_4$), 7.54 (d, ^3J(H,H) = 7.1 Hz, 2H, pyridine-*H*$_{3,5}$), 3.88 (d, ^2J(H,H) = 15. 4 Hz, 2H, C*H*HP*i*Pr$_2$), 3.72 (d, ^2J(H,H) = 15.4 Hz, 2H, C*H*HP*i*Pr$_2$), 2.56–2.40 (m, 4H, PC*H*(CH_3)$_2$), 1.57 (dd, ^3J(H,P) = 13.6 Hz, = 7.0 Hz, 6H, PCH(C*H*$_3$)$_2$), 1.44 (dd, ^3J(H,P) = 12.1 Hz, ^3J(H,H) = 6.6 Hz, 6H, PCH(C*H*$_3$)$_2$), 1.19 (dd, = 15.6, ^3J(H,H) = 7.1 Hz, 6H, PCH(C*H*$_3$)$_2$), 0.88 (dd, ^3J(H,P) = 16.0 Hz, ^3J(H,H) = 8.4 Hz, 6H, PCH(C*H*$_3$)$_2$), −25.59 ppm (t, ^2J(H,P) = 54.4 Hz, 1H, Fe-*H*); ^{31}P{^{1}H} NMR (162 MHz, [D_6]ethanol, 25 °C): δ = 85.88 (s, *P*-Fe-*P*), −141.31 ppm (sept, ^1J(P,F) = 709.2 Hz, *P*F$_6$); ESI-MS (pos., CH_3CH_2OH): *m*/*z* (%): 470.10 (30) [M^+], 452.15 (80) [{(*i*Pr-PNP)FeH(CO)$_2$}$^+$, decomp prod.], 378.15 (100) [{*i*Pr-PNP + K}$^+$, decomp prod.]; ESI-MS (neg., CH_3CH_2OH): 144.84 (100) [PF_6^-].

When the above reaction was performed in EtOH, followed by evaporation of the solvent, an orange brown solid was obtained, which was insoluble in non-polar organic solvents, but formed a yellow solution in acetone. The ^{1}H NMR showed a slightly shifted hydride signal at δ = −22.98 ppm together with the byproducts, which were also observed in alcoholic solvents (see below). It is likely that the coordinated EtOH is replaced by acetone under these conditions. Although free ethanol could not be detected by ^{1}H NMR spectroscopy, it is likely that it was removed

in vacuo. ^{1}H NMR (400 MHz, [D$_6$]acetone, 25 °C): δ = 7.89 (t, ^3J(H,H) = 7.7 Hz, 1H, pyridine-H_4), 7.61 (d, ^3J(H,H) = 7.7 Hz, 2H, pyridine-$H_{3,5}$), 3.87 (dvt, ^2J(H,H) = 17. 7 Hz, ^2J(H,P) = 4.6 Hz, 2H, CHHPiPr$_2$), 3.80 (dvt, ^2J(H,H) = 17.7 Hz, ^2J(H,P) = 3.5 Hz, 2H, CHHPiPr$_2$), 2.60–2.48 (m, 2H, PCH(CH$_3$)$_2$), 2.44–2.32 (m, 2H, PCH(CH$_3$)$_2$), 1.34–1.23 (m, 12H, PCH(CH_3)$_2$), 1.11 (dd, ^3J(H,P) = 13.6 Hz, ^3J(H,H) = 7.0 Hz, 6H, PCH(CH_3)$_2$), 0.99 (dd, ^3J(H,P) = 14.3 Hz, ^3J(H,H) = 6.8 Hz, 6H, PCH(CH_3)$_2$), −22.98 ppm (t, ^2J(H,P) = 51.3 Hz, 1H, Fe-H). ^{1}H{^{31}P} NMR (400 MHz, [D$_6$]acetone, 25 °C): δ = 7.89 (t, ^3J(H,H) = 7.7 Hz, 1H, pyridine-H_4), 7.61 (d, ^3J(H,H) = 7.7 Hz, 2H, pyridine-$H_{3,5}$), 3.87 (d, ^2J(H,H) = 17.3 Hz, 2H, CHHPiPr$_2$), 3.80 (d, ^2J(H,H) = 17.3 Hz, 2H, CHHPiPr$_2$), 2.60–2.47 (m, 2H, PCH(CH$_3$)$_2$), 1.30 (d, ^3J(H,H) = 7.4 Hz, 6H, PCH(CH_3)$_2$), 2.30–2.45 (m, 2H, PCH(CH$_3$)$_2$), 1.27 (d, ^3J(H,H) = 6.8 Hz, 6H, PCH(CH_3)$_2$), 1.11 (d, ^3J(H,H) = 7.3 Hz, 6H, PCH(CH_3)$_2$), 0.99 (d, ^3J(H,H) = 6.8 Hz, 6H, PCH(CH_3)$_2$), −22.98 ppm (s, 1H, Fe-H). ^{31}P{^{1}H} NMR (162 MHz, [D$_6$]acetone, 25 °C): δ = 94.76 (s, P-Fe-P), −141.08 ppm (sept, ^1J(P,F) = 707.2 Hz, PF$_6$).

After approximately 3–4 h in CD$_3$OD a significant amount of a new complex was observed in the ^{1}H and ^{31}P{^{1}H} NMR spectra. This complex gives rise to a triplet of doublets at δ = −11.66 ppm in the ^{1}H NMR spectrum for the hydride ligand (^2J(H,P) = 62.8 Hz, J(H,P) = 37.2 Hz) and was correlated to a triplet resonance at δ = 51.82 ppm and a doublet resonance at δ = 80.84 ppm in the ^{31}P{^{1}H} NMR (J(P,P) = 15.1 Hz) spectrum. The pattern of the signals in the ^{31}P{^{1}H} NMR spectrum together with the pattern of the hydride ligand in the ^{1}H NMR spectrum suggests that an ancillary phosphine ligand is bound to the iron center, in addition to the *i*Pr-PNP ligand. The nature of this complex is not clear.

Reaction of [(*i*Pr-PNP)FeH(CO)(BH$_4$)] with PhCHO and PhC(O)Me: As the H/D exchange of the hydride and partial exchange of the benzylic positions in the ligand are competitive in all the reactions investigated, benzaldehyde was used to generate the active species in spite of the low catalytic activity of **1** in the hydrogenation of this substrate. Generation of the active species using benzaldehyde is significantly faster than with acetophenone, allowing for characterization by 2D-NMR spectroscopy. The corresponding reactions with acetophenone were always used for comparison.

The following procedure was representative for the performed NMR experiments: [(*i*Pr-PNP)FeH(CO)(BH$_4$)] (**1**) (4.4 mg, 0.01 mmol) was suspended in CD$_3$OD (0.5 mL) and 1 equivalent of benzaldehyde (1.1 mg, 0.01 mmol) was added, followed by immediate analysis by NMR spectroscopy. Initially, three complexes were observed: the starting material [(*i*Pr-PNP)FeH(CO)(BH$_4$)] (**1**), a complex with a triplet signal at δ = −18.39 ppm for the hydride ligand and a broad resonance at δ = −5.71 ppm in the ^{1}H NMR spectrum (**1a**) and the cationic complex [(*i*Pr-PNP)Fe(H)(CO)(DOCD$_3$](PF$_6$) (**5**-CD$_3$OD) described above.

NMR data for **1a**: ^{1}H NMR (400 MHz, CD$_3$OD, 25 °C): δ = 7.91 (overlapped m, 1H, pyridine-H_4), 7.58 (overlapped m, 2H, pyridine-$H_{3,5}$), 3.79 (superimposed, 2H, CHHPiPr$_2$), 3.44 (d, ^2J(H,H) = 14.5 Hz, 2H, CHHPiPr$_2$), 2.45 (m, 2H, PCH(CH$_3$)$_2$), 2.18 (m, 2H, PCH(CH$_3$)$_2$), 1.42 (overlapped m, 6H, PCH(CH_3)$_2$), 1.18 (overlapped m, 12H, PCH(CH_3)$_2$), 0.89 (overlapped m, 6H, PCH(CH_3)$_2$), −5.71 (br, 4H, Fe-HBH_3), −18.39 ppm (t, ^2J(H,P) = 55.3 Hz, 1H, Fe-H); ^{31}P{^{1}H} NMR (162 MHz, CD$_3$OD, 25 °C): δ = 89.58 ppm (s).

^{1}H NMR measurements at different temperatures: The broad signal of the starting complex **1** started to attenuate at 243 K and was split into a broad three-proton resonance at δ = 0.06 ppm and a broad one-proton resonance at δ = −13.24 ppm, which was consistent with a η^1-coordination mode of the tetrahydridoborate ligand. The broad resonance at δ = −5.71 ppm of the tetrahydridoborate ligand in the newly formed complex (**1a**) started to attenuate at lower temperature at around 230 K and only at 178 K did a broad resonance at δ = −11.62 ppm for the bridging hydrogen atom appear again, while the reappearing three proton resonance of the terminal tetrahydridoborate hydrogen atoms was superimposed by the signal of complex **1**.

NMR data for **6b**-CD$_3$OD: ^{1}H NMR (400 MHz, CD$_3$OD, 25 °C): δ = −6.39 ppm (t, ^2J(H,P) = 44.9 Hz 1H, Fe-H); ^{31}P{^{1}H} NMR (162 MHz, CD$_3$OD, 25 °C): δ = 98.98 ppm (s).

NMR data for **6a**-CD$_3$CD$_2$OD: ^{1}H NMR (400 MHz, [D$_6$]ethanol, 25 °C): δ = −22.97 ppm (dd, ^2J(H,P) = 61.3 Hz, ^2J(H,P) = 47.2 Hz, 1H, Fe-H); ^{31}P{^{1}H} NMR (162 MHz, [D$_6$]ethanol, 25 °C): δ = 113.46 and 117.66 ppm (AB spin system, ^2J(P,P) = 143.6 Hz).

NMR data for **6b**-CD$_3$CD$_2$OD: ^{1}H NMR (400 MHz, [D$_6$]ethanol, 25 °C): δ = −6.40 (t, ^2J(H,P) = 43.6 Hz, 1H, Fe-H) ppm. ^{31}P{^{1}H} NMR (162 MHz, [D$_6$]ethanol, 25 °C): δ = 99.10 ppm (s).

Computational Details

All calculations were performed using Gaussian 09 (Revision B.01).[29] Two DFT exchange-correlation functionals were used. The first is the Perdew-Burke-Ernzerhof (PBE) generalized-gradient approximation (GGA) functional.[30] This was used for geometry optimizations. The second is Adamo and Barone's hybrid version of this functional (PBE0, also known as PBEh or PBE1PBE),[31] which was used for energy and solvation calculations.

Two basis set-RECP (relativistic effective core potential) combinations were used. The first, denoted SDD(d), is the combination of the Huzinaga-Dunning double-ζ basis set[32] on lighter elements with the Stuttgart-Dresden basis set-RECP combination[33] on transition metals; polarization functions (i.e., the D95(d) basis set) was used on second-row (i.e., phosphorus) atoms. The second is the Dunning cc-pVDZ basis set[34] (using the built-in cc-pVDZ basis set in Gaussian 09 for Fe). Geometry optimizations and frequency calculations were carried out using the former basis set while the energetics of the reaction were calculated at these geometries with the latter basis set.

When using the PBE functional, density fitting basis sets, specifically the fitting sets generated using the automatic generation algorithm implemented in Gaussian 09, were used in order to speed up the calculations.[35]

The accuracy of the DFT method was improved by adding the empirical dispersion correction as recommended by Grimme.[36] The older version (DFTD2)[36a] is available, with analytical gradients and Hessians, in Gaussian 09 and was used during geometry optimizations and frequency calculations; our version of Gaussian 09 was locally modified to allow for its use for any DFT functional rather than just the limited set included in the commercially available version. The newer, and more accurate, DFTD3 version[36b] was used as an a posteriori correction to the PBE0 energies obtained from Gaussian 09; a locally modified version of the stand-alone program written by Grimme was used.[37]

Bulk solvent effects were approximated by single point energy calculations using a polarizable continuum model (PCM),[38] specifically the integral equation formalism model (IEF-PCM)[38a,b,39] with ethanol as the solvent as in the experiments. Specifically, Truhlar's empirically parameterized version Solvation Model Density (SMD) was used.[40]

Geometries were optimized using the default pruned (75302) grid, while the "ultrafine" (i.e., a pruned (99590)) grid was used for energy and solvation calculations.

Acknowledgements

This research was supported by the European Research Council under the FP7 framework (ERC No 246837) and by the MINERVA Foundation. R.L. received a Post Doctoral Fellowship from the Deutsche Forschungsgemeinschaft (DFG). D.M. holds the Israel Matz Professorial Chair of Organic Chemistry.

[1] a) S. Enthaler, K. Junge, M. Beller, *Angew. Chem.* **2008**, *120*, 3363–3367; *Angew. Chem. Int. Ed.* **2008**, *47*, 3317–3321; b) C. Bolm, J. Legros, J. Le Paih, L. Zani, *Chem. Rev.* **2004**, *104*, 6217–6254; c) A. Correa, O. G. Mancheño, C. Bolm, *Chem. Soc. Rev.* **2008**, *37*, 1108–1117.

[2] a) R. Jana, T. P. Pathak, M. S. Sigman, *Chem. Rev.* **2011**, *111*, 1417–1492; b) W. M. Czaplik, M. Mayer, J. Cvengros, A. Jacobi von Wangelin, *ChemSusChem* **2009**, *2*, 396–417; c) B. D. Sherry, A. Fürstner,

Acc. Chem. Res. **2008**, *41*, 1500–1511; d) C.-L. Sun, B.-J. Li, Z.-J. Shi, *Chem. Rev.* **2011**, *111*, 1293–1314.

[3] a) R. H. Morris, *Chem. Soc. Rev.* **2009**, *38*, 2282–2291; b) S. Gaillard, J. Renaud, *ChemSusChem* **2008**, *1*, 505–509; c) C. Sui-Seng, F. Freutel, A. J. Lough, R. H. Morris, *Angew. Chem.* **2008**, *120*, 954–957; *Angew. Chem. Int. Ed.* **2008**, *47*, 940–943; d) A. Mikhailine, A. J. Lough, R. H. Morris, *J. Am. Chem. Soc.* **2009**, *131*, 1394–1395; e) S. Enthaler, B. Hagemann, G. Erre, K. Junge, M. Beller, *Chem. Asian J.* **2006**, *1*, 598–604; f) S. Zhou, S. Fleischer, K. Junge, S. Das, D. Addis, M. Beller, *Angew. Chem.* **2010**, *122*, 8298–8302; *Angew. Chem. Int. Ed.* **2010**, *49*, 8121–8125; g) J. Yang, T. D. Tilley, *Angew. Chem.* **2010**, *122*, 10384–10386; *Angew. Chem. Int. Ed.* **2010**, *49*, 10186–10188.

[4] a) S. C. Bart, E. Lobkovsky, P. J. Chirik, *J. Am. Chem. Soc.* **2004**, *126*, 13794–13807; b) S. C. Bart, E. J. Hawrelak, E. Lobkovsky, P. J. Chirik, *Organometallics* **2005**, *24*, 5518–5527; c) R. J. Trovitch, E. Lobkovsky, E. Bill, P. J. Chirik, *Organometallics* **2008**, *27*, 1470–1478.

[5] a) C. P. Casey, H. Guan, *J. Am. Chem. Soc.* **2007**, *129*, 5816–5817; b) C. P. Casey, H. Guan, *J. Am. Chem. Soc.* **2009**, *131*, 2499–2507.

[6] C. Sui-Seng, F. N. Haque, A. Hadzovic, A. Pütz, V. Reuss, N. Meyer, A. J. Lough, M. Zimmer-De Iuliis, R. H. Morris, *Inorg. Chem.* **2009**, *48*, 735–743.

[7] a) R. M. Bullock, *Chem. Eur. J.* **2004**, *10*, 2366–2374; b) R. M. Bullock in *Handbook of Homogeneous Hydrogenation* (Eds.: J. G. de Vries, C. J. Elsevier), Wiley-VCH, Weinheim, **2007**, Chapter 7; c) R. Noyori, T. Ohkuma, *Angew. Chem.* **2001**, *113*, 40–75; *Angew. Chem. Int. Ed.* **2001**, *40*, 40–73; d) N. B. Johnson, I. C. Lennon, P. H. Moran, J. A. Ramsden, *Acc. Chem. Res.* **2007**, *40*, 1291–1299.

[8] R. Langer, G. Leitus, Y. Ben-David, D. Milstein, *Angew. Chem.* **2011**, *123*, 2168–2172; *Angew. Chem. Int. Ed.* **2011**, *50*, 2120–2124.

[9] a) J. Zhang, G. Leitus, Y. Ben-David, D. Milstein, *J. Am. Chem. Soc.* **2005**, *127*, 10840–10841; b) C. Gunanathan, Y. Ben-David, D. Milstein, *Science* **2007**, *317*, 790–792; c) B. Gnanaprakasam, J. Zhang, D. Milstein, *Angew. Chem.* **2010**, *122*, 1510–1513; *Angew. Chem. Int. Ed.* **2010**, *49*, 1468–1471; d) J. Zhang, G. Leitus, Y. Ben-David, D. Milstein, *Angew. Chem.* **2006**, *118*, 1131–1133; *Angew. Chem. Int. Ed.* **2006**, *45*, 1113–1115; e) E. Balaraman, B. Gnanaprakasam, L. J. W. Shimon, D. Milstein, *J. Am. Chem. Soc.* **2010**, *132*, 16756–16758.

[10] a) T. Ohkuma, M. Koizumi, K. Muniz, G. Hilt, C. Kabuto, R. Noyori, *J. Am. Chem. Soc.* **2002**, *124*, 6508–6509; b) C. A. Sandoval, T. Ohkuma, K. Muniz, R. Noyori, *J. Am. Chem. Soc.* **2003**, *125*, 13490–13503; c) R. Guo, X. Chen, C. Elpelt, D. Song, R. H. Morris, *Org. Lett.* **2005**, *7*, 1757–1759; d) J. Zhang, E. Balaraman, G. Leitus, D. Milstein, *Organometallics* **2011**, *30*, 5716–5724.

[11] G. W. Schaeffer, J. S. Roscoe, A. C. Stewart, *J. Am. Chem. Soc.* **1956**, *78*, 729–733.

[12] R. Bau, H. S. H. Yuan, M. V. Baker, L. D. Field, *Inorg. Chim. Acta* **1986**, *114*, L27–L28.

[13] a) M. Koutmos, D. Coucouvanis, *Inorg. Chem.* **2004**, *43*, 6508–6510; b) M. Koutmos, I. P. Georgakaki, D. Coucouvanis, *Inorg. Chem.* **2006**, *45*, 3648–3656.

[14] a) C. A. Ghilardi, P. Innocenti, S. Midollini, A. Orlandini, *J. Organomet. Chem.* **1982**, *231*, C78–C80; b) C. A. Ghilardi, P. Innocenti, S. Midollini, A. Orlandini, *J. Chem. Soc. Dalton Trans.* **1985**, 605–609.

[15] a) M. P. Mehn, S. D. Brown, T. K. Paine, W. W. Brennessel, C. J. Cramer, C. J. Peters, L. Que, Jr., *Dalton Trans.* **2006**, 1347–1351; b) J. C. Vites, C. Eigenbrot, T. P. Fehlner, *J. Am. Chem. Soc.* **1984**, *106*, 4633–4635.

[16] a) A. C. Hillier, H. Jacobsen, D. Gusev, H. W. Schmalle, H. Berke, *Inorg. Chem.* **2001**, *40*, 6334–6337; b) G. Guilera, G. S. McGrady, J. W. Steed, N. Kaltsoyannis, *New J. Chem.* **2004**, *28*, 444–446.

[17] T. J. Marks, J. R. Kolb, *Chem. Rev.* **1977**, *77*, 263–293.

[18] a) P. J. Desrosiers, L. Cai, Z. Lin, R. J. Halpern, *J. Am. Chem. Soc.* **1991**, *113*, 4173–4184; b) G. J. Kubas, *Acc. Chem. Res.* **1988**, *21*, 120–128; c) G. J. Kubas, *Chem. Rev.* **2007**, *107*, 4152–4205; d) J. Eckert, G. J. Kubas, *J. Phys. Chem.* **1993**, *97*, 2378–2384.

[19] All complexes investigated in this study undergo H/D exchange of the hydrides and the benzylic position of the ligand.

[20] For details, see Supporting Information.

[21] a) M. Besora, A. Lledós, *Struct. Bonding (Berlin)* **2008**, *130*, 149–202; b) Z. Xu, Z. Lin, *Coord. Chem. Rev.* **1996**, *156*, 139–161.

[22] C. A. Sandoval, Y. Yamaguchi, T. Ohkuma, K. Kato, R. Noyori, *Magn. Reson. Chem.* **2006**, *44*, 66–75.

[23] a) M. A. Iron, E. Ben-Ari, R. Cohen, D. Milstein, *Dalton Trans.* **2009**, 9433–9439; b) L. Schwartsburd, M. A. Iron, L. Konstantinovski, Y. Diskin-Posner, G. Leitus, L. J. W. Shimon, D. Milstein, *Organometallics* **2010**, *29*, 3817–3827.

[24] S. W. Kohl, L. Weiner, L. Schwartzburd, L. Konstantinovski, L. J. W. Shimon, Y. Ben-David, M. A. Iron, D. Milstein, *Science* **2009**, *324*, 74–77.

[25] M. A. Iron, A. Sundermann, J. M. L. Martin, *J. Am. Chem. Soc.* **2003**, *125*, 11430–11441.

[26] a) G. Zeng, Y. Guo, S. Li, *Inorg. Chem.* **2009**, *48*, 10257–10263; b) E. Khaskin, M. A. Iron, L. J. W. Shimon, J. Zhang, D. Milstein, *J. Am. Chem. Soc.* **2010**, *132*, 8542–8543; c) L. Schwartsburd, M. A. Iron, L. Konstantinovski, E. Ben-Ari, D. Milstein, *Organometallics* **2011**, *30*, 2721–2729.

[27] a) S. Kozuch, S. Shaik, *Acc. Chem. Res.* **2011**, *44*, 101–110; b) A. Uhe, S. Kozuch, S. Shaik, *J. Comput. Chem.* **2011**, *32*, 978–985.

[28] A. Jansen, S. Pitter, *Monatsh. Chem.* **1999**, *130*, 783–794.

[29] Gaussian 09 (Revision B.01), M. J. Frisch, G. W. Trucks, H. B. Schlegel, G. E. Scuseria, M. A. Robb, J. R. Cheeseman, G. Scalmani, V. Barone, B. Mennucci, G. A. Petersson, H. Nakatsuji, M. Caricato, X. Li, H. P. Hratchian, A. F. Izmaylov, J. Bloino, G. Zheng, J. L. Sonnenberg, M. Hada, M. Ehara, K. Toyota, R. Fukuda, J. Hasegawa, M. Ishida, T. Nakajima, Y. Honda, O. Kitao, H. Nakai, T. Vreven, J. A. Montgomery, Jr., J. E. Peralta, F. Ogliaro, M. Bearpark, J. J. Heyd, E. Brothers, K. N. Kudin, V. N. Staroverov, R. Kobayashi, J. Normand, K. Raghavachari, A. Rendell, J. C. Burant, S. S. Iyengar, J. Tomasi, M. Cossi, N. Rega, J. M. Millam, M. Klene, J. E. Knox, J. B. Cross, V. Bakken, C. Adamo, J. Jaramillo, R. Gomperts, R. E. Stratmann, O. Yazyev, A. J. Austin, R. Cammi, C. Pomelli, J. W. Ochterski, R. L. Martin, K. Morokuma, V. G. Zakrzewski, G. A. Voth, P. Salvador, J. J. Dannenberg, S. Dapprich, A. D. Daniels, O. Farkas, J. B. Foresman, J. V. Ortiz, J. Cioslowski, D. J. Fox, Gaussian, Inc., Wallingford CT, **2009**.

[30] a) J. P. Perdew, K. Burke, M. Ernzerhof, *Phys. Rev. Lett.* **1996**, *77*, 3865–3868; b) J. P. Perdew, K. Burke, M. Ernzerhof, *Phys. Rev. Lett.* **1997**, *78*, 1396.

[31] C. Adamo, V. Barone, *J. Chem. Phys.* **1999**, *110*, 6158–6170.

[32] T. H. Dunning, Jr., P. J. Hay in *Modern Theoretical Chemistry, Vol. 3*, Plenum, New York, **1976**, pp. 1–28.

[33] M. Dolg in *Effective Core Potentials. In Modern Methods and Algorithms of Quantum Chemistry, Vol. 1*, John von Neumann Institute for Computing, Jülich (Germany), **2000**, pp. 479–508.

[34] T. H. Dunning, Jr., *J. Chem. Phys.* **1989**, *90*, 1007–1023.

[35] a) B. I. Dunlap, *J. Chem. Phys.* **1983**, *78*, 3140–3142; b) B. I. Dunlap, *J. Mol. Struct. (THEOCHEM)* **2000**, *529*, 37–40.

[36] a) T. Schwabe, S. Grimme, *Phys. Chem. Chem. Phys.* **2007**, *9*, 3397–3406; b) S. Grimme, J. Antony, S. Ehrlich, H. Kreig, *J. Chem. Phys.* **2010**, *132*, 154104.

[37] http://toc.uni-muenster.de/DFTD3/, accessed July 13, **2010**.

[38] a) B. Mennucci, J. Tomasi, *J. Chem. Phys.* **1997**, *106*, 5151–5158; b) E. Cancès, B. Mennucci, J. Tomasi, *J. Chem. Phys.* **1997**, *107*, 3032–3041; c) M. Cossi, V. Barone, B. Mennucci, J. Tomasi, *Chem. Phys. Lett.* **1998**, *286*, 253–260; d) M. Cossi, G. Scalmani, N. Rega, V. Barone, *J. Chem. Phys.* **2002**, *117*, 43–54.

[39] a) B. Mennucci, E. Cancès, J. Tomasi, *J. Phys. Chem. B* **1997**, *101*, 10506–10517; b) J. Tomasi, B. Mennucci, E. Cancès, *J. Mol. Struct. (THEOCHEM)* **1999**, *464*, 211–226.

[40] A. V. Marenich, C. J. Cramer, D. G. Truhlar, *J. Phys. Chem. B* **2009**, *113*, 6378–6396.

[41] X. Yang, *Inorg. Chem.* **2011**, *50*, 12836–12843.

[42] a) I. Langmuir, *Trans. Faraday Soc.* **1922**, *17*, 621–654; b) C. N. Hirshelwood, *The Kinetics of Chemical Change*, Clarendon Press, Oxford, **1940**.
[43] D. D. Eley, E. K. Rideal, *Nature* **1940**, *146*, 401–402.
[44] R. J. Baxter, P. Hu, *J. Chem. Phys.* **2002**, *116*, 4379–4381 and references therein.
[45] S. Takebayashi, N. Dabral, M. Miskolzie, S. H. Bergens, *J. Am. Chem. Soc.* **2011**, *133*, 9666–9669.

Received: January 15, 2012
Published online: ■■ ▮▮, 0000

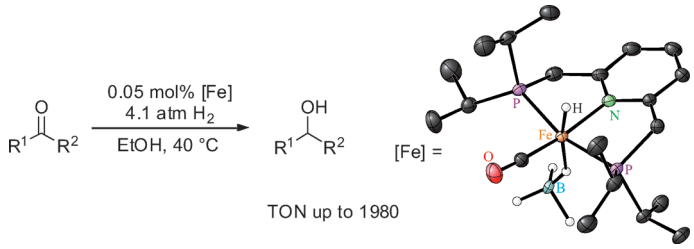

An excellent catalyst for the hydrogenation of ketones under mild and base-free conditions has been obtained with the new hydrido tetrahydrido complex [(*i*Pr-PNP)Fe(H)(CO)(BH_4)]. Detailed NMR investigations indicate that the tetrahydridoborate ligand has to dissociate prior to ketone reduction. Based on DFT calculations a mechanism involving concerted ketone coordination and dual hydrogen transfer from the PNP arm and the coordinated ethanol to the ketone is indicated.

Homogeneous Catalysis

*R. Langer, M. A. Iron, L. Konstantinovski, Y. Diskin-Posner, G. Leitus, Y. Ben-David, D. Milstein** ..... ▮▮▮▮–▮▮▮▮

Iron Borohydride Pincer Complexes for the Efficient Hydrogenation of Ketones under Mild, Base-Free Conditions: Synthesis and Mechanistic Insight